UNIVERSITY OF THESSALY
SCHOOL OF ENGINEERING
DEPARTMENT OF MECHANICAL ENGINEERING

Simulation of a hybrid SOFC/GT system for cogeneration purposes

THESIS
submitted in partial fulfillment of the requirements
for the degree of Master of Science
of the department of Mechanical Engineering
University of Thessaly

by

Diamantis Bakalis

Dipl. Mechanical Engineer

Approved:

Assist. Prof. A. G. Stamatis, Thesis Advisor

Volos, October 2010

Εγκρίθηκε από τα Μέλη της Τριμελούς Εξεταστικής Επιτροπής:

Πρώτος Εξεταστής (Επιβλέπων)	Δρ. Αναστάσιος Σταμάτης Επίκουρος Καθηγητής, Τμήμα Μηχανολόγων Μηχανικών, Πανεπιστήμιο Θεσσαλίας
Δεύτερος Εξεταστής	Δρ. Αναστάσιος Σταματέλλος Καθηγητής, Τμήμα Μηχανολόγων Μηχανικών, Πανεπιστήμιο Θεσσαλίας
Τρίτος Εξεταστής	Δρ. Ερρίκος Σταπουντζής Αναπληρωτής Καθηγητής, Τμήμα Μηχανολόγων Μηχανικών, Πανεπιστήμιο Θεσσαλίας

CONTENTS

Nomenclature

D	Diffusion coefficients
D_m	Mean diameter
E	Potential
F	Faraday constant
g	Gibbs free energy
h	Enthalpy
j	Current density
k	Factor
$\dot{m}$	Mass flow
MW	Molecular weight
n	Mole
N	Rotational speed
P	Pressure
p	Partial pressure
PR	Pressure ratio
R_g	Gas constant
r	Electrode pore radious
S/C	Steam to carbon ratio
T	Temperature
t	Thickness
TIT	Turbine inlet temperature
U	Utilization factor
V	Voltage
v	Fuller diffusion coefficient
w	width
W	Power
y	Molar fraction
ε	Porosity

η	Efficiency
ξ	Tortuosity
ρ	Resistivity

Subscripts

a	Air
A	anode
C	Cathode
c	Compressor
DP	Design point
E	Electrolyte
eff	Effective
f	Fuels
gen	Generator
GT	Gas turbine
HS	Hybrid system
Int	Interconnection
m	mechanical
op	Operating
rel	Relative
t	Turbine

LIST OF FIGURES

Acknowledgements

First of all I want to thank my advisor Dr. Anastassios Stamatis, without his guidance, support and patience; the work would never have been conducted. It was a great pleasure to work with him.

Special thanks to other members of my supervising committee Dr. Anastassios Stamatelos and Dr. Herricos Stapountzis.

1. Introduction

Nowadays highly effective energy conversion systems are developed, in order to meet the needs of increasing energy demands, the decreasing amount of fossil energy resources and the necessity of low pollutants and greenhouse gases emission.

Fuel cells are electrochemical power generation devices which directly converts the fuel chemical energy into electrical energy. Their emissions are very low compared to traditional power generation systems. Among fuel cells, solid oxide fuel cells (SOFC) have a higher thermal efficiency and are operated with very high temperatures (about 1000°C). Another important advantage SOFCs is that the high temperature exhaust gases can be used as heat source for other thermally activated devices.

The hybrid solid oxide fuel cell gas turbine (SOFC-GT) systems have attracted the interest from many researches worldwide. A large number configurations and cycles have been proposed and investigated. Both theoretical and experimental analyses of those systems have exhibit their excellence in efficient energy conversion and in low environmental impact.

Although, hybrid SOFC-GT systems are in research stage, in the future are going to play a significant role in the energy market. Their future potential applications are in large central station power plants operated on a variety of fuels, local commercial and various distributed generation applications.

The main objective of this thesis is to develop a robust simulation model in AspenPlus software for a hybrid SOFC-GT system. The hybrid system consists of a high temperature SOFC, based on the tubular configuration developed by Siemens Power Generation Inc, and a recuperated small gas turbine (GT) validated using data for the Capstone C30. The developed model was used in order to study the part load performance of the system

1.1 Contents of this thesis

Chapter 2 contains a literature review about micro cogeneration systems and the micro turbine based cogeneration systems. After that the main modeling techniques for gas turbines are referred and the Capstone C30 micro turbine is presented. Also a review about fuel cells is done and the Siemens tubular SOFC is presented.

Chapter 3 includes the developed models of Capstone C30 micro turbine, SOFC stack and hybrid system.

Chapter 4 presents the part load performance of the hybrid system and the effect of various operating parameters on system performance.

2. Literature review

Cogeneration is the simultaneous production of heat and electricity from a single fuel source. Traditionally, the cogeneration was implemented in large electricity plants to increase the overall efficiency, by capturing the waste heat and use it for heating or cooling. Nowadays, there is the trend for distributed power generation, small cogeneration (microcogeneration) systems are available to energy market and can satisfy the energy needs of a house or larger buildings such as hotels, hospitals etc.

One of the most popular types of microcogeneration systems are the micro turbine based systems, because of their benefits which are mentioned in the following paragraphs. The main components of those systems are a small turboshaft engine for electricity production and a heat exchanger in order to capture the heat of the exhaust gases. A further improvement for that type of cogeneration systems is feasible when completed with fuel cells.

2.1 Micro-cogeneration systems

Cogeneration is the simultaneous production of power and heat, from a single fuel, both of which are used. Also, cogeneration is known as 'Combined Heat and Power' (CHP). Microcogeneration is the same thing with cogeneration but in smaller scale, and it is used in residential and small commercial applications.

Figure 2-1 presents the basic concept of microcogeneration. A prime mover, such as a gas turbine, converts the chemical energy of fuel to mechanical energy and drives a generator which produces electrical power. The waste heat from the prime mover can be recovered by a heat exchanger to produce hot water or to heat a building and to drive thermally activated devices, such as absorption chillers and desiccant devices.

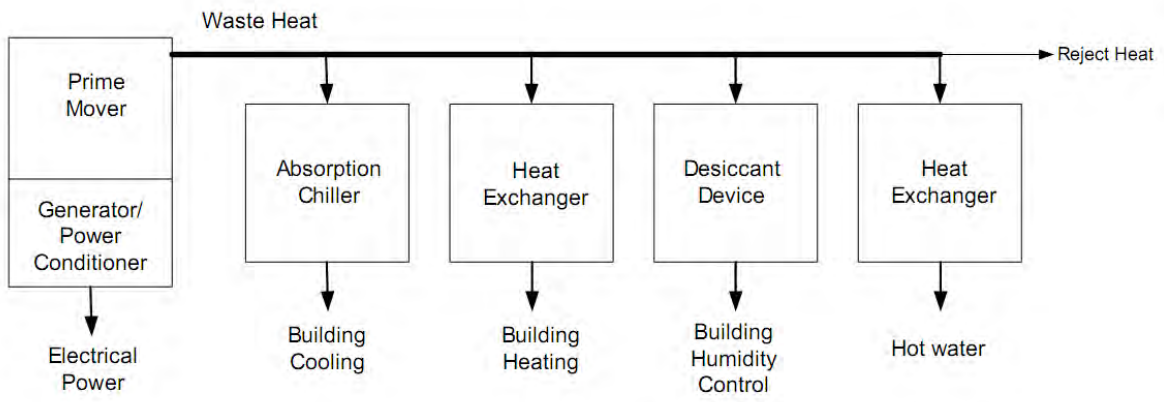

Figure 2-1 Schematic of a microcogeneration system,[1]

In cogeneration system achieved efficiencies of energy conversion over 80% compared to an average of 30-35% for a conventional fossil fuel fired electricity generation systems, [2].

The main benefits of cogeneration are:

- *Increased efficiency of energy conversion and use*, since a small amount of the initial chemical energy (fuel) is rejected to the environment.
- *Lower emissions.* The high efficiency of cogeneration systems requires smaller fuel amount, so the emissions, especially of CO_2 the main greenhouse gas, are lower.
- *Large cost savings,* making the cogeneration plants an attractive investment for industrial and commercial users, and offering affordable heat for domestic users. In those systems the payback period or three to five years can be achieved.
- *Decentralized electricity production,* where the plant is designed to meet the local consumers demand, avoiding transmission loses and increasing the flexibility of system use.

Cogeneration systems utilize various technologies for energy conversion. Among these technologies the prime mover of the system plays a significant role in the system performance, reliability and flexibility. In Table 2-1 are presented the characteristics and parameter of prime movers in cogeneration systems, [3].

	Steam turbines	Diesel engines	Spark ignition engines	Combustion turbines	Micro-turbines	Stirling engines	Fuels cells
Capacity range	50kW-500MW	5kW-20MW	3kW-6MW	250kW-50MW	15-300kW	1kW-15MW	5kW-2MW
Fuel used	Any	Gas, propane, distillate oils, biogas	Gas, biogas, liquid fuels, propane	Gas, propane, distillate oils, biogas	Gas, propane, distillate oils, biogas	Any (gas, alcohol butane, biogas)	Hydrogen and fuels containing hydrocarbons
Efficiency electrical[%]	7-20	35-45	25-43	25-42	15-30	~40	37-60
Efficiency overall [%]	60-80	65-90	70-92	65-87	60-85	65-85	85-90
Power to heat ratio	0.1-0.5	0.8-2.4	0.5-0.7	0.2-0.8	1.2-1.7	1.2-1.7	0.8-1.1
Output heat temperature[°C]	Up to 540	370-540	370-540	Up to 540	200-350	60-200	260-370
Noise	Loud	Loud	Loud	Loud	Fair	Fair	Quiet
CO_2 emissions [kg/MWh]		650	500-620	580-680	720	672	430-490
NO_x emissions [kg/MWh]		10	0.2-1.0	0.3-0.5	0.1	0.23	0.005-0.01
Availability [%]	90-95	95	95	96-98	98	N/A	90-95
Part load performance	Poor	Good	Good	Fair	Fair	Good	Good
Life cycle [years]	25-35	20	20	20	10	10	10-20
Average cost investment [$/kW]	1000-2000	340-1000	800-1600	450-950	900-1500	1300-2000	2500-3500
Operating and maintenance costs [$/kWh]	0.004	0.0075-0.015	0.0075-0.015	0.0045-0.0105	0.01-0.02	N/A	0.007-0.05

Table 2-1 Characteristics and parameters of prime movers in cogeneration systems

2.1.1 Micro turbine based cogeneration systems

Micro turbines are miniatures of larger gas turbine engines. The recent years there is a growing interest in that type of engines in micro cogeneration systems because their unique characteristics compared with other prime movers (Table 2-1).

Micro turbines operate on the same thermodynamic cycle, known as the Brayton cycle, as larger gas turbines [4]. In this cycle, atmospheric air is compressed, heated and then expanded, with the excess power produced by the expander over that consumed by the compressor used for power generation. The power produced by an expansion turbine and consumed by a compressor is proportional to the absolute temperature of the gas passing through those devices. Consequently, it is advantageous to operate the expansion turbine at the highest practical temperature consistent with economic materials and to operate the compressor with inlet airflow at as low temperature as possible. As technology advances permit higher turbine inlet temperature, the optimum pressure ratio also increases. Higher temperature and pressure ratios result in higher efficiency and specific power. Thus, the general trend in gas turbine advancement has been toward a combination of higher temperatures and pressures. However, micro turbine inlet temperatures are generally limited to 1250 K or below to enable the use of relatively inexpensive materials for the turbine wheel and to maintain pressure rations at a comparatively low 3.5 to 4.0.

Micro turbines are small gas turbines, most of which feature an internal heat exchanger called a recuperator [4]. In a micro turbine, a radial flow compressor compresses the inlet air that is then preheated in the recuperator using heat from the engine exhaust. Next, the heated air from the recuperator mixes with fuel in the combustor and hot combustion gas expands through the turbine. The turbine turns the compressor and, in single shaft models, turns the generator as well. Finally, the recuperator uses the exhaust of the turbine to preheat the air from the compressor.

A simple diagram of the thermodynamic cycle on which operate the micro turbines is presented in Figure 2-2. The use of the recuperator (or the regenerator) increases the efficiency of the simple Brayton cycle, since the recuperator utilize a portion of energy of the exhaust gases to preheat the air entering in the combustion chamber. This, in turn, decreases the amount of fuel required for the same power output

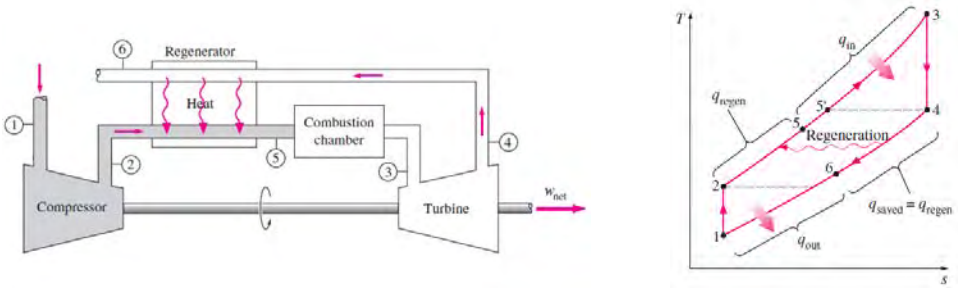

Figure 2-2 A gas turbine engine with recuperator (regenerator) and T-s diagram

A typical micro turbine installation (Figure 2-3) embodying the following features, [3, 5]: 1) single stage radial compressor and turbine, 2) single shaft design, 3) multi-fuel combustion capability, 4) high effective compact recuperator, 5) simple control system and 6) air bearings to support the high speed rotor.

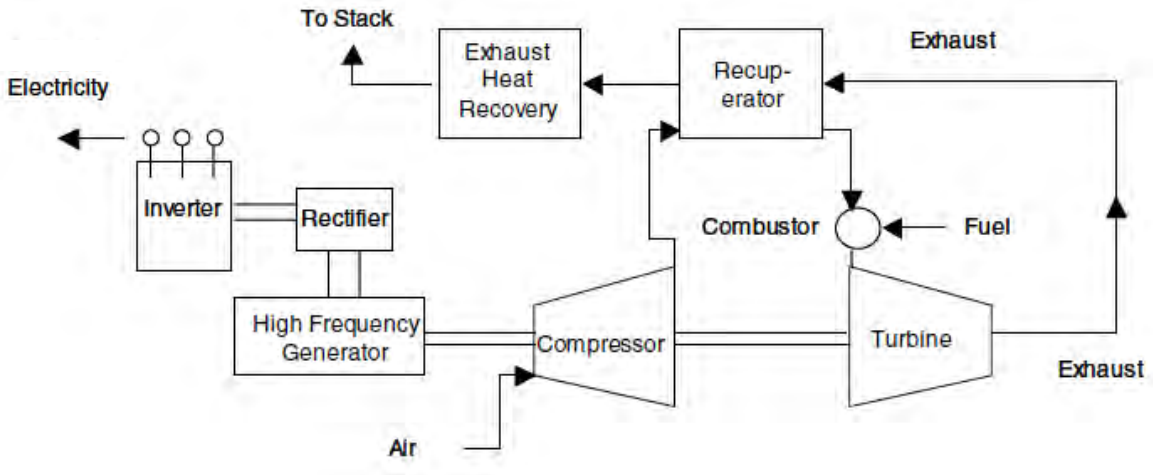

Figure 2-3 Schematic of a recuperated micro turbine based cogeneration system, [4].

Micro turbines offer a number of advantages, making them appropriate to cover the electrical and heating power demands of residential, commercial or institutional buildings. The characteristics which make them an attractive solution are the compact size, low weight, small number of moving parts, low emissions levels, high-grade waste heat, low noise and vibration, low maintenance requirements, short delivery time and the fact that small-scale units can combine large system of multiple units, [2, 3].

The main disadvantages are the high first cost, the low electrical efficiency, the fair part load performance which is sensitive to changes in ambient conditions, [3].

2.1.2 Simulation of micro turbines

There are many works about performance prediction and simulation of small gas turbine operation with engine models, [6-8]. Engine models are defined as mathematical descriptions of the physical behavior of a turbine engine.

All the simulation aim at computing the fluid state in different locations of the mainstream in the engine, from these results, mainly mass flow, temperature and pressure, it is possible to derive powers, thrusts, fuel consumptions and all characteristic parameters of the components.

The simulation model can be split into different categories according to the level of discretization of space. In Table 2-2 are summarized the different categories of simulation models, [9].

Type	Description
0-D	Average fluid characteristics at discrete positions (generally at inlets-outlets of each component
1-D	Average fluid characteristics at sections
2-D	There is symmetry of revolution for the stream
3-D	No simplifications – use the complete equations of conservation

Table 2-2 Different types of simulation models

2.1.2.1 0-D Models

These models are the most widely spread in the world of turbo-machinery for many reasons[9]:

- Historically, they were the first kind of performance model that was used.
- They do not require a detailed description of the engine geometry. Thus they can be used very early in the engine development.

- The engine description is simple and close to reality by considering it as a set of black boxes, one for each major component of the engine.
- The calculation methods are simple because the number of unknowns needed by the modeling is reduced, the goal being to compute the fluid characteristics only at the interfaces of the black boxes. The number of unknowns has the same order of magnitude as the number of individual components considered as black boxes.
- The calculation methods are natural because the fluid characteristics are computed plane by plane, or station by station, in the same order as the one used by the fluid to pass through the engine. The calculation begins at the air inlet, continues with the compressors, the combustion chamber, the turbines, and ends with the exhaust.
- Thanks to the simplicity of 0-D models, they can be run on all computer types, from the small portable PC to the workstation or the main frame. This is a very useful feature of 0-D models, because of the wide range of people who can have to run engine performance models. Such models constitute a common tool for the designer, the integrator, the customer; and the engine designer. As the main model provider, the engine designer finds issuing customer decks, based on the same approach as the one he uses for development, very convenient. This results in time and cost savings and quality gains.

2.1.2.2 0-D modeling technique

In order to develop the mathematical model, the overall engine is split in its components – subsystems and numerical model developed for each one. Each subsystem constitutes a component of the engine which performs a specific operation. Thereinafter, these individual models are merged to provide the overall system model. The resultant mathematical model is a system of equations which must be solved to predict the system behavior.

The micro turbines usually are divided in four subsystems:

- Compressor
- Recuperator
- Burner
- Turbine

The generator and power condition systems are taken into account by incorporating constant values for their efficiencies.

The compressor and turbine are modeled through a performance map, relating the mass flow, the efficiency, the pressure ratio and the rotational speed of the compressor for a range of operating conditions. The inlet and outlet conditions of those components are interrelated through the definition equations, the performance maps and equations of conservation.

Modeling of the burner is easier than modeling of rotating components. The burner is considered as a black box that receives hot compressed air from the recuperator and fuel. The combustion is usually modeled as a heat addition at quasi-constant pressure. The real added heat depends on the burning efficiency of the combustor.

The recuperator is a two stream heat exchanger. Its performance is determined with the effectiveness which is the ratio of the air temperature rise to the ideal value, the latter being the difference between the gas and air inlet temperatures.

Except from the previous parameters of the engine components, the boundary conditions (i.e. the ambient conditions) and two control variables must me specified in order to be able the calculation of the engine performance.

2.1.2.3 Control methods of micro turbines

In micro turbines the part load operation usually made as follows

- By **constant rotational speed** and reduction of fuel flow or turbine inlet temperature. Always two parameters must be controlled from the user, when fuel flow is determined from the user the turbine inlet temperature arises from the solution of system of equations and vice-versa.
- By **variable rotational speed** and constant turbine inlet temperature. That type of part load operation is the more preferred since the engine operates more efficiently [10].

2.1.3 Capstone C30 micro turbine

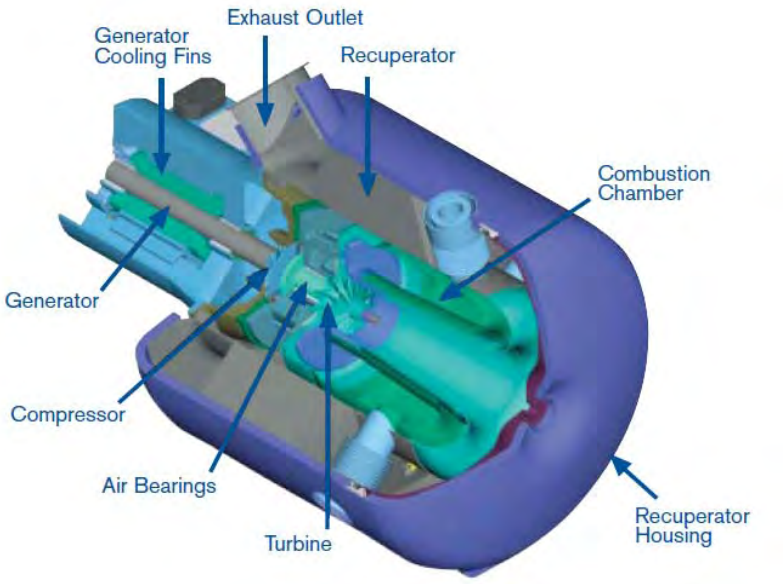

Figure 2-4 Capstone C30 micro turbine generator

The micro turbine which is referred in this thesis is the C30 manufactured by the Capstone Turbine Corporation. The Capstone C30 micro turbine system is a compact, ultra low emissions generator providing up to 30kW of power and 85kW of heat for combined heat and power applications. The system incorporates a compressor, recuperator, combustor, turbine and permanent magnet generator. The rotating components are mounted on a single shaft, supported by patented air bearings, that spin at up to 96000rpm. This is the only moving part of the microturbine. The generator is cooled by inlet air flow. The system uses no oil, lubricants, coolants or other hazardous materials, and has no pumps, gearbox or other mechanical subsystems. The system achieves ultra low *NOx* performance with no post-combustion catalysts or other cleanup devices or chemicals.

2.2 Fuel cells

2.2.1 Operating principles of fuel cells

The fuel cell is one of the main components of the investigated system. Fuel cells are electrochemical devices that convert the chemical energy of a reaction directly into electrical energy. In Figure 2-1 is shown the operating principle of a fuel cell, [11].

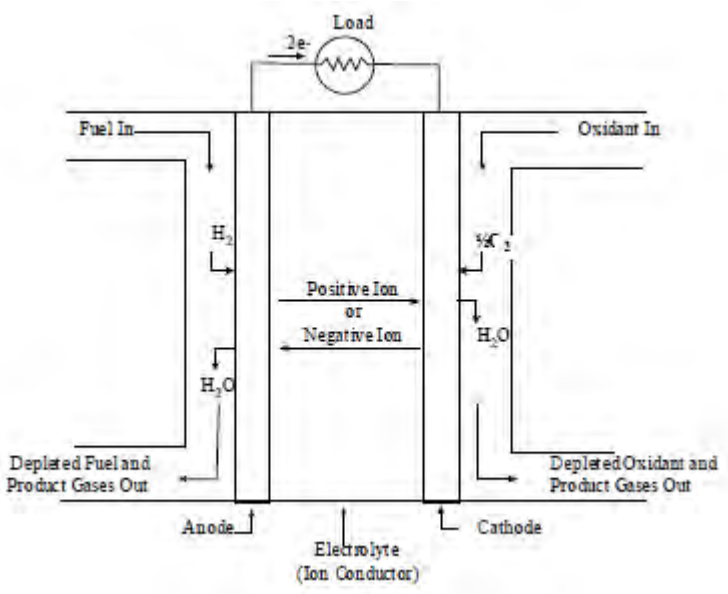

Figure 2-5 Operating principle of fuel cells

In a typical fuel cell, hydrogen fuel is fed to the anode (negative electrode) and an oxidant (oxygen) is fed to the cathode (positive electrode). Hydrogen indirect reacts with the oxygen to produce electrical power and water which is the by-product of the reaction.

Usually the classification of fuel cells is done according the kind of electrolyte being used, [12]. These include alkaline fuel cells (AFC), phosphoric acid fuel cells (PAFC), molten carbonate fuel cells (MCFC), zinc air fuel cells (ZAFC), proton exchange/polymer electrolyte membrane fuel cells (PEMFCs), solid oxide fuel cells (SOFC) and photonic ceramic fuel cells (PCFCs), which their required operating temperature vary widely.

In the Table 2-3 are presented the types of fuel cells are considered as viable systems for the present and near future, [13].

Among the fuel cells presented in Table 2-3, the SOFC can operate at high temperatures. The high operating temperature of that fuel cell, leads in high temperatures of fuel cell exhaust, so the high energy content of fuel cell exhaust can produce significant amount of mechanical power when expanded in a turbine. This characteristic makes the SOFC appropriate to be incorporated in gas turbine cycles.

Fuel cell type	Mobile ion	Operating temperature	Applications and notes
Alkaline (AFC)	OH^-	50-200°C	Used in space vehicles, e.g. Apollo, Shuttle.
Proton exchange membrane (PEMFC)	H^+	30-100°C	Vehicles and mobile applications, and for lower power CHP systems
Phosphoric acid (PAFC)	H^+	~200°C	Large numbers of 200kW CHP systems in use
Molten carbonate (MCFC)	CO_3^{2-}	~650°C	Suitable for medium to large scale CHP systems, up to MW capacity
Solid Oxide (SOFC)	O^{2-}	500-1000°C	Suitable for all sizes of CHP systems, 2 kW to multi-MW.

Table 2-3 Data for different types of fuel cells

2.2.2 Solid oxide fuel cells

In Figure 2-6 is presented the operating principle of the SOFC, [14]. In order a hydrogen-rich fuel (e.g. natural gas) to be useful by a fuel cell, it must be reformed to hydrogen (H_2) (Equation 2-1). This higher hydrocarbons and a small amount of methane (CH_4) are converted to hydrogen, carbon monoxide and carbon dioxide according to the stream reforming reaction (Equation 2-1) and water gas shift reaction (Equation 2-2).

$$C_nH_m + nH_2O \rightarrow nCO + \left(\frac{m}{2} + n\right)H_2 \qquad \textbf{Equation 2-1}$$

$$CO + H_2O \rightarrow CO_2 + H_2$$ **Equation 2-2**

At high operating temperature of the SOFC, the direct oxidation of the CO and CH_4 contained in the prereformed fuel is feasible without a catalyst, but the direct oxidation of these fuels is less favored than the water gas shift of CO to H_2 and reforming of CH_4 to H_2, [11] It is a commons system analysis practice to assume that H_2, the more readily oxidized fuel, is the only fuel electrichemicaly reacting [15]. It is fortunate that converting CO and CH_4 to equivalent H_2, and then reacting within the cell simplifies analysis while accurately predicting the electrochemical behavior of the fuel cell. The H_2 calculated to be produced from CO and CH_4, along with any H_2 in the supply system is referred as equivalent H_2.

The electrochemical reactions occurring in SOFC are [11]:

At the cathode

$$\tfrac{1}{2} O_2 + 2e^- \rightarrow O^{2-}$$ **Equation 2-3**

and at the anode

$$\begin{aligned} &H_2 + O^{2-} \rightarrow H_2O + 2e^- \\ &CO + O^{2-} \rightarrow CO_2 + 2e^- \\ &CH_4 + 4O^{2-} \rightarrow 2H_2O + CO_2 + 8e^- \end{aligned}$$ **Equation 2-4**

The electrons are conducted through an external electric circle, while the oxygen ions are conducted through the electrolyte.

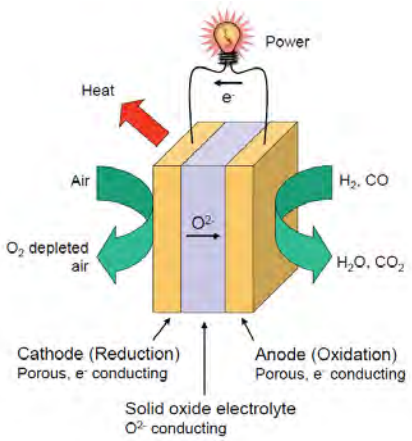

Figure 2-6 Operating principle of SOFC

The ideal performance of a fuel cell is defined by its Nernst potential represented as cell voltage. The Nernst equation provides a relationship between the ideal standard potential (E^o) for the cell reaction and the ideal equilibrium potential (E) at other temperatures and partial pressures of reactants and products. Once the ideal potential at standard conditions is known, the ideal voltage can be determined at the other temperatures and pressures through the use of the following equation:

$$E = E^0 + \frac{RT}{2F}\ln\left(\frac{P_{H_2}P_{O_2}^{1/2}}{P_{H_2O}}\right) \qquad \textbf{Equation 2-5}$$

According to Nernst equation for hydrogen reaction, the ideal cell potential at a given temperature can be increased by operating at higher pressure. The ideal standard potential of an H_2/O_2 fuel cell is 1.229 volts with liquid water product and 1.18 volts with gaseous water product [11]. In Figure 2-7 shows the relation of E^o to cell temperature. Because the figure shows the potential of higher temperature fuel cells, the ideal potential corresponds to a reaction where the water product is in gaseous state. Hence, E^o is less than 1.229 at standard conditions when considering gaseous water product.

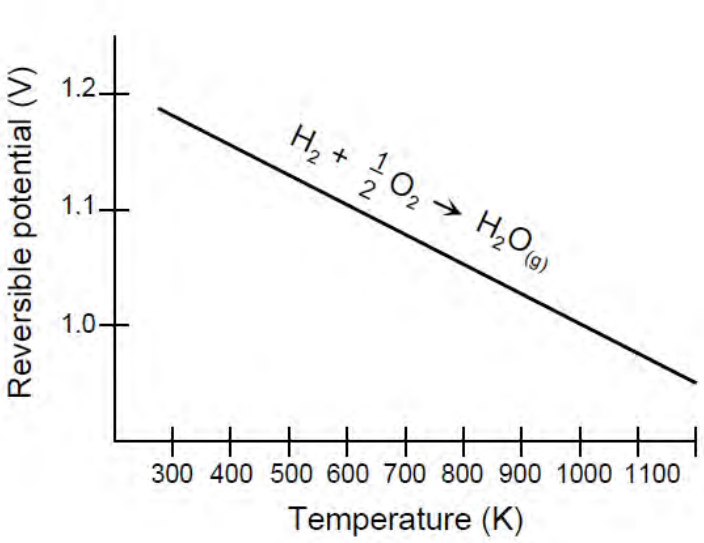

Figure 2-7 H_2/O_2 fuel cell ideal potential as a function of temperature, [11].

The actual gas voltage of a SOFC is less than the ideal potential because of irreversible losses including [11]:

- *Activation Polarization* is present when the rate of an electrochemical reaction at an electrode surface is controlled by sluggish electrode kinetics. In other words, activation polarization is directly related to the rates of electrochemical reactions. There is a close similarity between electrochemical and chemical reactions in that both involve an activation barrier that must be overcome by the reacting species.
- *Ohmic Polarization (losses)* occur because of resistance to the flow of ions in the electrolyte and resistance to flow of electrons through electrode materials. The dominant ohmic losses, through the electrolyte are reduced be decreasing the electrode separation and enhance the ionic conductivity of the electrolyte.
- *Concentration Polarization.* As a reactant is consumed at the electrode by electrochemical reaction, there is a loss of potential due to the inability of the surrounding material to maintain the initial concentration of the bulk fluid. That is, a concentration gradient is formed. Several processes may contribute to concentration polarization: slow diffusion in the gas phase in the electrode pores, solution/dissolution of reactants/products into/out the electrolyte, or diffusion or reactants/products through the electrolyte to/from the electrochemical reaction site.

There are several studies [16-18] concerning the developing of complex simulation models that predict the performance of a fuel cell based on the details of the stack design and operating conditions and using fundamental physical phenomena. That approach is complicated and the corresponding models demand heavy computations. A simpler approach is to use the current/voltage characteristic of the fuel cell at reference operating conditions in order to obtain a reference value for the voltage. Calculation of the actual cell voltage value, is then performed by semi-empirical correlations accounting for the differences due to the real operating conditions [19].

The performance of fuel cells is affected by operating variables (e.g. temperature, pressure, gas composition, reactant utilizations, current density) and other factor (impurities, cell life) that influence the ideal cell potential and the magnitude of the voltage losses described above. The effect of pressure and temperature of an ideal fuel cell is discussed previously. Reactant utilization and gas composition have major impact on cell efficiency. It is apparent from Nernst equation (Eq. 2-5) that fuel and oxidant gases containing higher partial pressures of electrochemical reactants produce a higher cell voltage.

Fuel utilization factor refers to the fraction of the fuel that reacts electrochemically to the total fuel introduced into a fuel cell. Because the H_2 assumed that is the only reactant involved in the electrochemical reaction, the utilization factor is given from the following equation:

$$U_f = \frac{n_{H_2,in} - n_{H_2,out}}{n_{H_2,in}} = \frac{n_{H_2,consumed}}{n_{H_2,in}} \qquad \textbf{Equation 2-6}$$

Air utilization factor is defined similarly with the fuel utilization factor. It is the ratio of the oxygen extracted from the air flow to oxidize the fuel to the total oxygen introduced to the cell (Eq. 2-7). For a cell of assigned size and active surface area, and with an assigned inlet air flow (coming for example, from a compressor), any variation of U_a is generated by a proportional variation of the number of oxygen ions conducted by the electrolyte. This number is then proportional to a variation of the cell current density and overall current output, [19].

$$U_a = \frac{n_{O_2,in} - n_{O_2,out}}{n_{O_2,in}} = \frac{n_{O_2,consumed}}{n_{O_2,in}}$$ **Equation 2-7**

Another parameter that affects the performance of a fuel cell is the stem-to-carbon ratio (SCR ratio). This parameter defined as the ratio between the number of the H_2O molecules and the number of the *C*-atoms of combustible components [19]. It must have an appropriate value in order to avoid the carbon deposition in the fuel channel. It is given from the following equation

$$SCR = \frac{n_{H_2O}}{n_{CO} + n_{CH_4} + 2 \times n_{C_2H_6} + 3 \times n_{C_3H_8} + \cdots}$$ **Equation 2-8**

The current density is defined as the current per unit area of electrode surface. This operating parameter is one of the most important for fuel cells and has significant effects on the cell voltage and efficiency.

2.2.3 Siemens-Westinghouse tubular SOFC

The fuel cell type which is presented in this work is the SOFC built by Siemens – Westinghouse Power Company. The specific type is the most developed SOFC in terms of accumulated operating hours and production facilities, [20].

In Figure 2-8 is presented a schematic view of Siemens – Westinghouse SOFC. The cell tube is closed at one end. For cell operation, oxidant (air or oxygen) is introduced through an alumina injector tube positioned inside the cell. The oxidant is discharged near the closed end of the cell and flows through the annular space formed by the cell and the coaxial injector tube. Fuel flows on the outside of the cell from the closed end and is electrochemically oxidized while flowing to the open end of the cell generating electricity. At the open end of the cell, the oxygen-depleted air exits the cell and is combusted with the partially depleted fuel. Typically, 50-90% of the fuel is utilized in the electrochemical cell reaction. Part of the

depleted fuel is re-circulated in the fuel stream and the rest is combusted to preheat incoming air and/or fuel. The exhaust gas from the fuel cell is at 600-900°C depending the operating conditions, [21].

As mentioned in the section 2.2.2 the SOFC can be fed with a fuel rich in hydrogen. Usually the used fuel is desulfurized natural gas at larger pressure than the cell operating pressure, [22]. The natural gas is introduced as the primary fluid in a jet pump or ejector which withdraws depleted fuel from the depleted fuel plenum and mixes it with the incoming natural gas. The higher hydrocarbons and a small amount of the methane are reformed during the pass of mixture through an adiabatic pre-reformer. The stream leaving the pre-reformer is routed to the top of the in-stack reformers where it flows downward through a catalytically active space to the fuel distribution plenum.

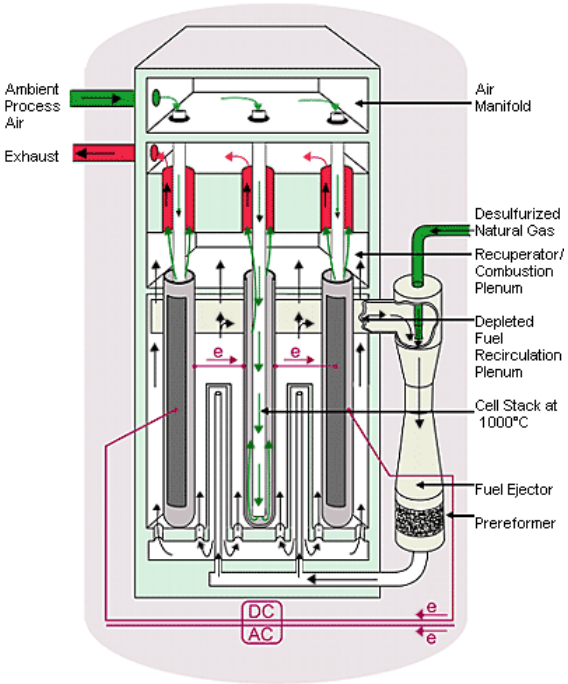

Figure 2-8 Schematic view of Siemens-Westinghouse SOFC, [23]

2.3 Hybrid power generation systems

A hybrid heat engine results from the fusion of a heat engine with a non-heat engine based cycle. The term combined cycle, which refers to similar arrangements, is reserved for the combination of two or more heat engines. The resulting product or the integration of a gas turbine and a fuel cell is referred as a hybrid system[24].

Hybrid heat engines are power generation systems in which a heat engine, such as a gas turbine, in combined with a non heat engine, such as a fuel cell. The resulting system exhibits a synergism in which the combination performs with an efficiency that far exceeds that which can be provided by either system alone (Figure 2-10). Thus the combination performs better than the sum of its parts. This attribute, combined with an inherent low level of pollutant emission, suggests that hybrid systems are likely to serve as the next generation of advanced power generation systems.

A micro gas turbine combined with SOFC represents a power cycle suggested in many studies. Those types of combined systems are called hybrid power generation systems (Figure 2-9), as mentioned previously. A micro gas turbine system operating with Brayton cycle is capable of efficiencies of ~30% and a simple SOFC power system can achieve efficiencies at the 50% level. By incorporating the previous systems into a hybrid the achievable efficiencies are about 60-70%, [20]. Another advantage of the hybrid systems is the low levels of pollutant emissions. The CO_2 content in exhaust gases is extremely low because of the high fuel economy of hybrid system. Since the higher amount of fuel is reacted in the SOFC stack, the NO_x concentrations in the system exhaust are the typically low SOFC values, [25]. The SO_x emissions are practical zero since the fuel is desulfurized to preclude the reactions of sulfur and its compounds with the anode catalyst.

In a hybrid system with a recuperated gas turbine the pressurized air that exits the compressor is preheated in a heat exchanger which utilizes the thermal energy of exhaust gases. Then the air enters in the fuel cell stack where reacts electrochemically with the fuel and produce electrical energy and thermal energy since the overall process in the stack is exothermic. The high temperature exhaust gases from the stack, which consist of unutilized reformed natural gas and depleted air, are driven to the burner where residual fuels and a small amount of fresh fuel react with the depleted air from the cathode compartment. The combusted gas mixture is expanded in the turbine the mechanical power is produced. This

power in used to drive the compressor and the rest to drive an electrical generator to produce additional electrical power.

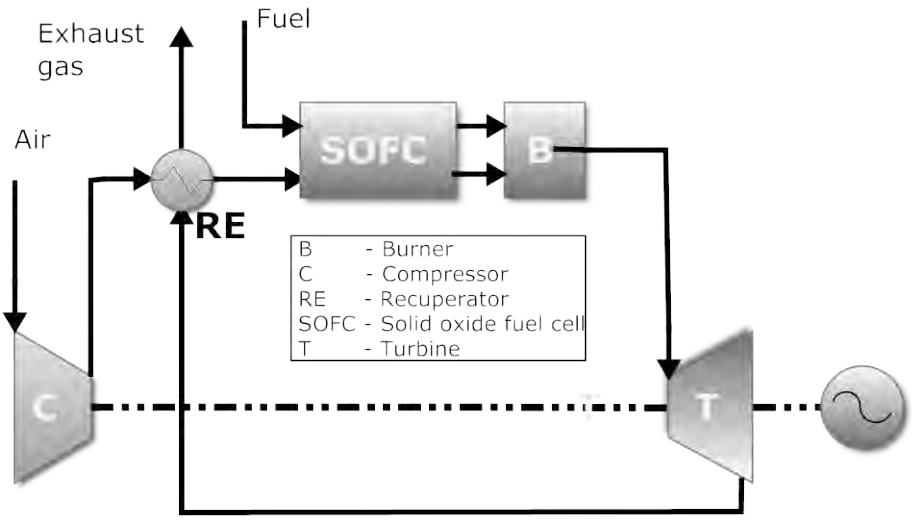

Figure 2-9 Hybrid system layout

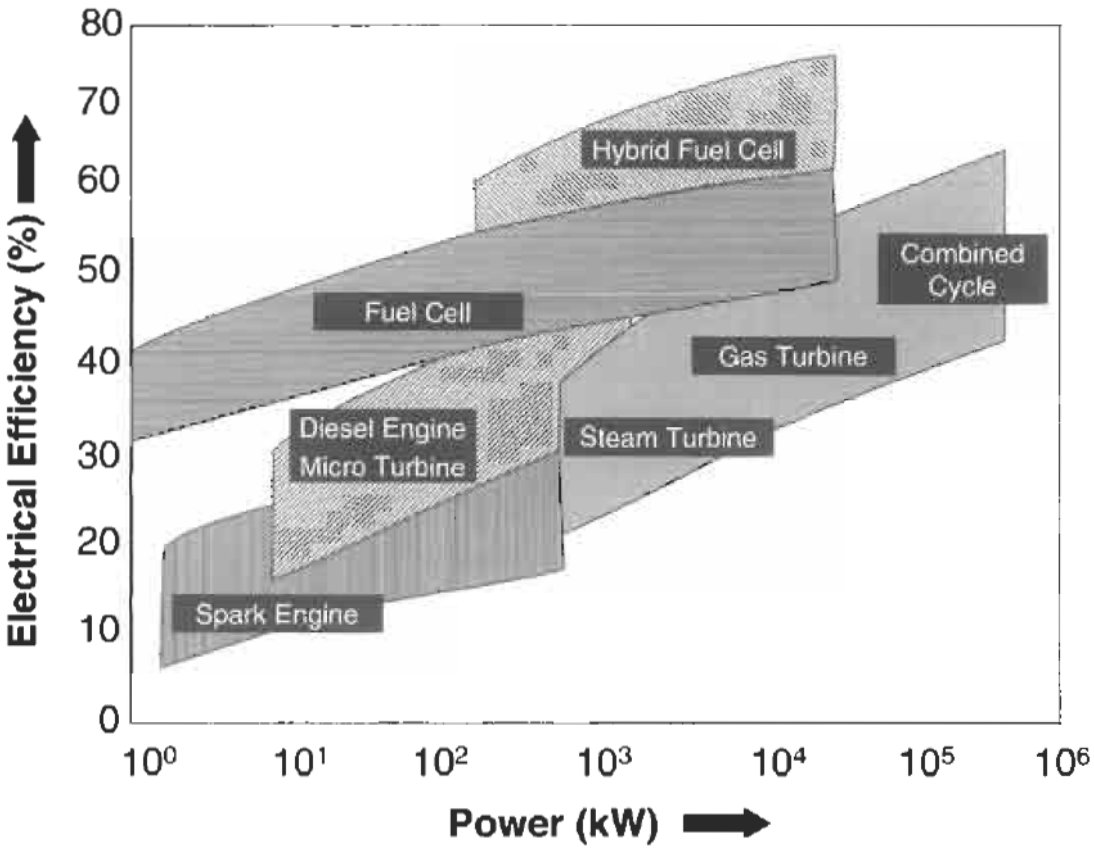

Figure 2-10 The electrical efficiency versus size for various power systems, adapted from [21].

3. Model development

3.1 Simulation software

The models used in the present thesis are developed in AspenPlus simulation software, [26]. AspenPlus is a commercially available process simulator for process analysis. The AspenPlus is based on "blocks" corresponding to unit operation such as compressor, reactors, heat exchanges etc. The blocks are interconnected using material, heat and work streams in order to construct a complete process flowsheet. AspenPlus contains several thermodynamic, physical and chemical property databases so it can simulate a wide range of processes and generate accurate simulation result. Besides the built in unit operation blocks AspenPlus offers the option to write your own unit operation models as Fortran subroutines. The Fortran user models can be used either as blocks or to perform complicated calculations.

AspenPlus has been used for many researchers in order to study the complicated energy plants. Adrain et al [27] used AspenPlus in order to develop a model of a micro gas turbine, and study the performance at high ambient temperatures with a view to integrating it with thermally activated cooling technologies. Zheng and Furimsky [28] simulated a natural gas fired gas/steam turbine combined cycle cogeneration plant. Kuchonthara et al [29] studied the a combined power generation system consisting of a solid oxide fuel cell (SOFC) and a gas turbine with steam and heat recuperation.

3.2 Fuel cell model

As mentioned in section 2.2.3 the fuel cell model is based on the tubular internal reforming SOFC technology developed by Siemens-Westinghouse. The considered model produces 100kWe. The unit employs 1152 commercial-size SOFCs in its cell stack, with as effective length 1500mm, a diameter of 22mm, a wall thickness about 2mm and an active area of about 834cm^2. When operating at atmospheric pressure, 85% utilization factor and 1000°C, the electrochemical process can achieve approximately 160W power output per cell, [15, 16, 30].

AspenPlus which is widely used software in industry and research was used to model the SOCF stack. There is no built in block that can represent a SOFC. A common approach to overcome that limitation is to develop a SOFC stack model in a programming language and link it to AspenPlus as a *UserModel,* [31, 32]. An alternative method proposed by Zhang et al.[15], where using AspenPlus built in model blocks they developed a simulation model able to provide detailed performance data of the SOFC operation. The model was validated using literature data of a Siemens-Westinghouse 100kWe class tubular internal reforming SOFC stack. The methodology of Zhang et al., was adapted from other researchers in order to simulate complicated energy plants. Meyer et al. [33] designed a simple bioenergy system, in AspenPlus, consisting of a high temperature SOFC integrated with an allothermal biomass gasification process and used that as an example to evaluate the environmental impact of energy conversion systems. Also, Doherty et al. [34] using AspenPlus developed a biomass gasification – SOFC combined heat and power plant, capable to predict the system performance under various operating conditions and using several fuels.

The SOFC model used in this thesis adapted from reference [15]. The AspenPlus SOFC model flowsheet is presented in Figure 3-1. Fresh fuel fed to the SOFC stack mixes with recycled anode gas containing the electrochemical reaction products (H_2O, CO_2 and some amount of unreacted H_2 and CO). Then this mixed stream is fed to the prereformers through the ejector. In the prereformers, the higher hydrocarbons and a small amount of methane in the natural gas are reformed according the reactions described from equations 2-1 and 2-2. At the anode the CO and CH_4 contained in the prereformed fuel are shifting and reformed to H_2 respectively according the reactions described from equations 3-1 and 3-2. Thus the H_2 is the only fuel electrochemically reacting.

$$CH_4 + H_2O \Leftrightarrow CO + 3H_2 \qquad \text{(Methane stream reforming)} \qquad \textbf{Equation 3-1}$$

$$CO + H_2O \Leftrightarrow CO_2 + H_2 \qquad \text{(Water-gas shift reaction)} \qquad \textbf{Equation 3-2}$$

The SOFC stack air inlet is preheated by the hot exhaust from the afterburner and enters the cell cathode to provide oxygen for the electrochemical reaction. After undergoing the chemical and electrochemical reactions, part of the depleted fuel gases recycles to mix with the

fresh fuel and provide steam for the prereforming reactions. The rest of the depleted fuel gases enter the combustion plenum and react with the oxygen in the depleted air

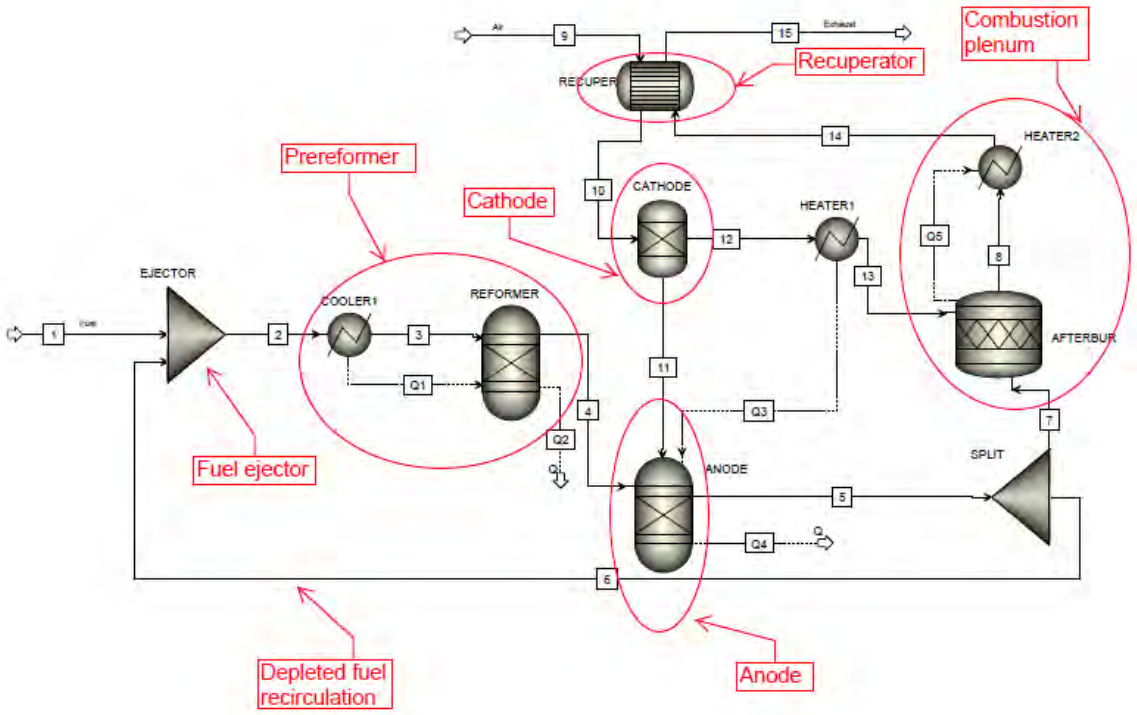

Figure 3-1 SOFC model AspenPlus flowsheet

The SOFC model performs heat and mass balances and considers the ohmic, activation and concentration losses for the voltage calculation. The system model predicts thermodynamic conditions and composition of all internal flow streams, voltage current and efficiency.

The assumptions for the simulation of the model are presented in Table 3-1.

Fuel inlet composition	CH_4 81.3%, C_2H_6 2.9%, C_3H_8 0.4%, C_4H_{10} 0.2%, N_2 14.3%, CO 0.9%
Cell operating temperature	1000°C
Cell operating pressure	1.08 bar
Power output (DC)	120kW
Active area	96.1 m^2 (1152 cells)
Cell exhaust temperatures (stream 13 and 15)	910°C
Inlet air temperature (stream 9)	630°C
Inlet fuel temperature (stream 1)	200°C
Afterburner efficiency	100%
DC to AC inverter	92%
Overall fuel utilization factor	85%
S/C ratio	2.5
Ejector fresh fuel pressure ratio	3
Temperature difference between the outlet of cold and hot stream in the "RECUPER" block	10°C
Pressure drops inside the SOFC	0
SOFC thermal losses	2%

Table 3-1 Assumptions of SOFC model

The voltage was calculated applying the methodology used by Doherty et al. [34]. First is applied the widely known Nernst equation to determine open circuit voltage and then the various losses, including ohmic, activation and concentration, are subtracted from the open circuit voltage in order to determine the actual voltage. Below, the voltage calculation equations are presented.

- Reversible Nernst voltage

$$V_N = -\frac{\Delta \bar{g}_f}{2F} + \frac{R_g T_{op}}{2F} \ln \frac{p_{H_2} {p_{O_2}}^{0.5}}{p_{H_2O}} \qquad \textbf{Equation 3-3}$$

- Ohmic loss

$$V_{Ohm\_A} = \frac{j \rho_A (A \pi D_m)^2}{8 t_A} \qquad \textbf{Equation 3-4}$$

$$V_{Ohm\_C} = \frac{j\rho_C(\pi D_m)^2}{8t_C} A[A + 2(1 - A - B)]$$ **Equation 3-5**

$$V_{Ohm\_E} = j\rho_E t_E$$ **Equation 3-6**

$$V_{Ohm\_Int} = j\rho_{Int}(\pi D_m)\frac{t_{Int}}{w_{Int}}$$ **Equation 3-7**

- Activation loss

$$\frac{1}{R_{Act\_A}} = \frac{2F}{R_g T_{op}} k_A \left(\frac{p_{H_2}}{p^o}\right)^m \exp\left(\frac{-E_A}{R_g T_{op}}\right)$$ **Equation 3-8**

$$\frac{1}{R_{Act\_C}} = \frac{4F}{R_g T_{op}} k_C \left(\frac{p_{O_2}}{p^o}\right)^m \exp\left(\frac{-E_C}{R_g T_{op}}\right)$$ **Equation 3-9**

$$V_{Act\_C} = jR_{Act\_C}$$ **Equation 3-10**

$$V_{Act\_C} = jR_{Act\_C}$$ **Equation 3-11**

- Concentration loss

$$V_{Conc\_A} = -\frac{R_g T_{op}}{2F} \ln\left[\frac{1 - \frac{R_g T_{op}}{2F} \cdot \frac{t_A}{D_{An(eff)} y^o{}_{H_2} P_{SOFC}} j}{1 + \frac{R_g T_{op}}{2F} \cdot \frac{t_A}{D_{An(eff)} y^o{}_{H_2O} P_{SOFC}} j}\right]$$ **Equation 3-12**

$$V_{Conc\_C} = -\frac{R_g T_{op}}{4F} \ln\left[\frac{\frac{P_{SOFC}}{\delta_{O_2}} - \left(\frac{P_{SOFC}}{\delta_{O_2}} - y^o{}_{O_2} P_{SOFC}\right) \exp\left[\frac{R_g T_{op}}{4F} \cdot \frac{\delta_{O_2} t_C}{D_{Cat(eff)} P_{SOFC}} j\right]}{y^o{}_{O_2} P_{SOFC}}\right] \quad \textbf{Equation 3-13}$$

- Actual voltage

$$V = V_N - (V_{Ohm} + V_{Act} + V_{Conc}) \quad \textbf{Equation 3-14}$$

The concentration losses was modeled using Eq. (3-12) and (3-13). Only diffusion transport in the electrodes (gases in pores) was taken into account, the convective phenomena were ignored. The Eq. (3-12) and (3-13) were derived using Fick's law of diffusion and both ordinary and Knudsen diffusion were considered. Ordinary diffusion occurs when the pore diameter of the material is large in comparison to the mean free path of the gas molecules, on the other hand, when the pores of the material are small in comparison with the mean free path of the molecules then occurs Knudsen diffusion. Both types of diffusion were taken into account in determination of effective diffusion coefficients for the anode and cathode. The Knudsen diffusion coefficient for the anode and cathode gases is given from Eq. (3-15).

$$D_{A,K} = 97r\left(\frac{T_{op}}{MW_A}\right)^{0.5} \left(m^2/s\right) \quad \text{where } (A = H_2, H_2O, O_2 \text{ or } N_2) \quad \textbf{Equation 3-15}$$

The effective Knudsen diffusion coefficient is given by

$$D_{A,K(eff)} = D_{A,K}(\varepsilon / \xi) \quad \text{where } (A = H_2, H_2O, O_2 \text{ or } N_2) \quad \textbf{Equation 3-16}$$

The ordinary binary diffusion coefficients for both anode and cathode were calculated using the semi-empirical correlation proposed by Fuller et al. [35].

$$D_{AB} = 1 \times 10^{-7} T_{op}^{1.75} \left(\frac{1}{MW_A} + \frac{1}{MW_B} \right)^{0.5} \frac{1}{P\left(\nu_A^{1/3} + \nu_B^{1/3} \right)^2} \left(m^2/s \right) \quad \textbf{Equation 3-17}$$

Where the subscripts A and B indicate the binary gas mixtures of O_2-N_2 at the cathode and H_2-H_2O at the anode. The Fuller diffusion volumes v_i are given in Table 3-2. The effective ordinary diffusion is arises similarly with Knudsen diffusion.

$$D_{AB(eff)} = D_{AB}(\varepsilon / \xi) \quad \textbf{Equation 3-18}$$

The overall effective diffusion coefficient for each gas is calculated using Eq. (3-19)

$$\frac{1}{D_{A(eff)}} = \frac{1}{D_{AB(eff)}} + \frac{1}{D_{A,K(eff)}} \quad \textbf{Equation 3-19}$$

Finally, the anode and cathode diffusion coefficients are:

$$D_{An(eff)} = \frac{P_{H_2O}}{P_{SOFC}} D_{H_2(eff)} + \frac{P_{H_2}}{P_{SOFC}} D_{H_2O(eff)} \quad \textbf{Equation 3-20}$$

$$D_{Cat(eff)} = D_{O_2(eff)} \quad \textbf{Equation 3-21}$$

The parameter δ_{O2} in Eq.(3-13) is given from the following relation

$$\delta_{O_2} = \frac{D_{O_2,K(eff)}}{D_{O_2,K(eff)} + D_{O_2N_2(eff)}}$$

The parameters that appeared in Eq. (3-3) – (3-18) are given in Table 3-2

Geometry parameters	
Cell length (m)	1.5
Cell outer diameter (m)	0.022
Anode thickness t_A (m)	0.0001
Cathode thickness t_C (m)	0.0022
Electrolyte thickness t_E (m)	0.00004
Interconnection thickness t_{Int} (m)	0.000085
Interconnection width w_{Int} (m)	0.009
Material properties	
Anode resistivity ρ_A (Ωm)	$2.98\times10^{-5}\exp(-1392/T_{op})$
Cathode resistivity ρ_C (Ωm)	$8.114\times10^{-5}\exp(600/T_{op})$
Electrolyte resistivity ρ_E (Ωm)	$2.94\times10^{-5}\exp(10350/T_{op})$
Interconnection resistivity ρ_{Int} (Ωm)	0.025
Ohmic loss	
A/B	0.804/0.13
Activation loss	
Pre-exponential factor k_A/k_C (A/m^2)	$2.13\times10^{8}/1.49\times10^{10}$
Slope m	0.25
Activation energy E_A/E_C (J/mol)	110000/160000
Concentration loss	
Electrode pore radius r (m)	5×10^{-7}
Electrode porosity ε/tortuosity ξ	0.5/5.9
Fuller diffusion volume v_{H2}	7.07
Fuller diffusion volume v_{H2O}	12.7
Fuller diffusion volume v_{O2}	16.6
Fuller diffusion volume v_{N2}	17.9

Table 3-2 SOFC parameters

3.3 Gas turbine model

The AspenPlus software is an excellent modeling tool for advanced power cycles. It has been used in study of gas and steam turbine power plants, [36, 37]. In the following sections are described the basic components of the micro turbine simulation model in AspenPlus.

In Figure 3-2 are presented the basic components of a micro turbine recuperated cycle. It utilizes a compressor, a recuperator, a burner, a turbine and a generator. The heart of the micro turbine is the compressor turbine package which is commonly mounted on a single shaft along with the electric generator, [4]. Small gas turbine engines are more likely to have single stage radial flow compressors and turbine, since achieve higher pressure ratios with lower flow rates compared to lower stage pressure ratios and higher flow rates in axial flow

turbomachineries, [38]. Also, radial turbomachineries offer higher efficiencies since the surface and end wall losses are minimum, [2]. Recuperators are heat exchangers that use the hot turbine exhaust gas to preheat the compressed air going into the burner, thereby reducing the fuel needed to heat the compressed air to the turbine inlet temperature. In the burner the heated air from the recuperator mixes with the fuel in the combustor and hot combustion gas expands through the turbine.

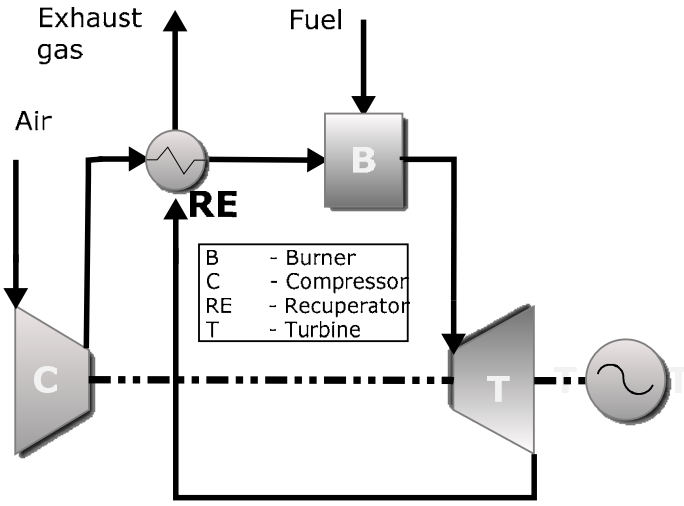

Figure 3-2 Basic components of the micro turbine system

3.3.1 Compressor

AspenPlus contains a common block for the simulation of compressor and turbine. The block is named *Compr* and is shown in Figure 3-3. The *Compr* is used to change steam pressure when energy-related information, is needed or known. It can simulate a compressor, by specifying the related information such as pressure ratio, efficiency, performance curves etc. *Compr* can be fed with performance curves or to supply a user performance curve subroutine written in Fortran programming language. The user subroutine can calculate either parameters related with the exit pressure, or the developed head or the power. The *Compr* block cannot handle performance curves for a turbine.

In the specific model it was chosen to supply a user performance curve subroutine written in Fortran programming language. The AspenPlus provide a ready subroutine template which can be used as a driver for the calculations in performance curves. The specific method was chosen because of the performance curves it can be fed to the subroutine with an ASCII file in tabular format so it is easy to modify the performance curves using a spreadsheet software. Also there were ready in house Fortan subroutines for interpolations in performance curves.

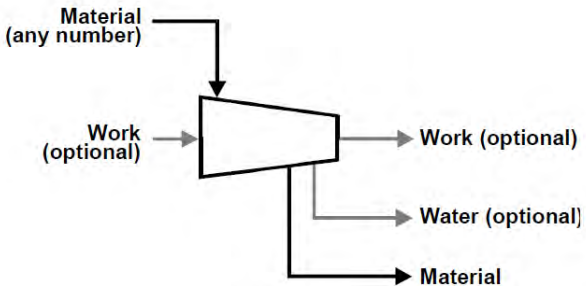

Figure 3-3 AspenPlus *Compr* block

The compressor performance map (curves) was chosen from the included maps with GasTurb package. The map was scaling using the following relations [39]

$$PR = \frac{PR_{D.} - 1}{PR_{M.D.} - 1}(PR_{M.} - 1) + 1 \qquad \textbf{Equation 3-22}$$

$$\dot{m} = \frac{\dot{m}_{D.}}{\dot{m}_{M.D.}}\dot{m}_{M.} \qquad \textbf{Equation 3-23}$$

$$\eta = \frac{\eta_{D.}}{\eta_{M.D.}}\eta_{M.} \qquad \textbf{Equation 3-24}$$

Where:

D. = design point map values of scaled components

M. = arbitrary map values

M.D = design point map values of original components

The scaled compressor performance curves are presented in the Figures Figure 3-4 and Figure 3-5. The corrected mass flow is given by the following equation:

$$\dot{m}_c = \dot{m}\frac{\sqrt{\Theta}}{\delta}$$ **Equation 3-25**

and the corrected speed:

$$N_c = N\sqrt{\Theta}$$ **Equation 3-26**

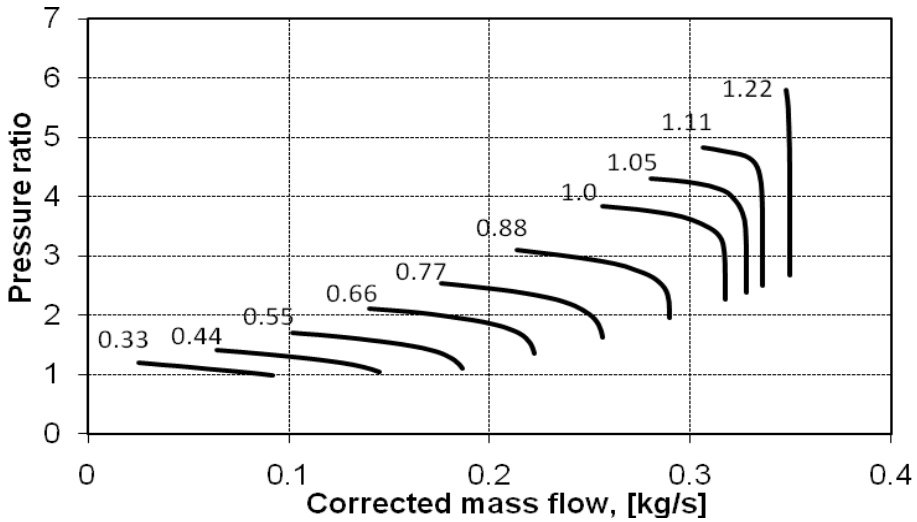

Figure 3-4 Compressor performance map (pressure ratio)

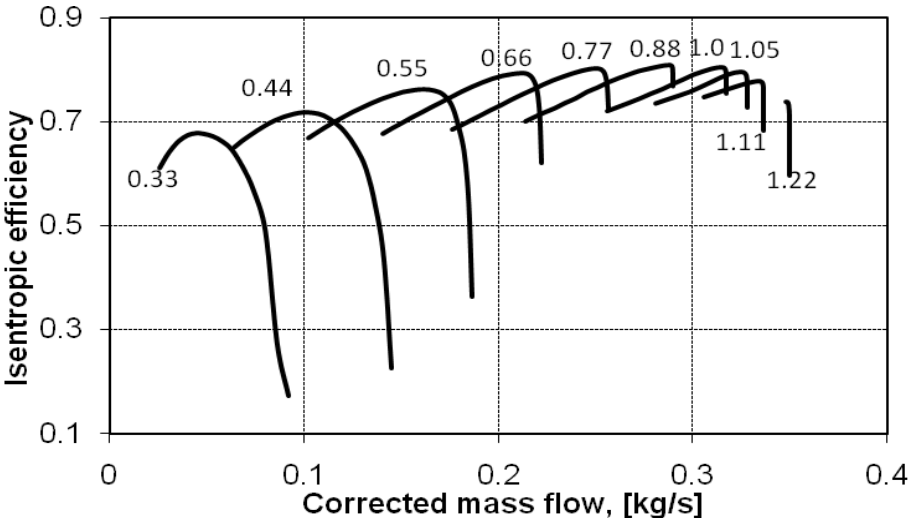

Figure 3-5 Compressor performance map (efficiency curves)

3.3.2 Turbine

As mentioned in the section 3.3.1 the *Compr* block cannot handle performance curves for a turbine. So it is decided to develop a Fortran subroutine in order to simulate the turbine performance.

The inputs to the turbine model are:

- The mass flow
- The rotational speed
- The inlet temperature
- The inlet pressure
- And the performance curves

Given the previous parameters it is feasible to calculate all the related parameters regard the turbine performance. The user model is expressed by following groups of equations, [40]:

- Definition equations:

  Pressure ratio:

$$PR = \frac{P_{in}}{P_{out}} \qquad \textbf{Equation 3-27}$$

  Isentropic efficiency:

$$\eta = \frac{h_{in} - h_{out}}{h_{in} - h_{out,is}} \qquad \textbf{Equation 3-28}$$

- Relations of characteristic parameters (in tabular form)

$$PR = PR(\dot{m}_t, N_t) \qquad \textbf{Equation 3-29}$$

$$\eta = \eta(\dot{m}_t, N_t) \qquad \textbf{Equation 3-30}$$

  Where:

$$N_t = \frac{N}{N_{des}} \frac{\sqrt{T_{in,des}}}{\sqrt{T_{in}}} \quad \rightarrow \text{(speed parameter)} \qquad \textbf{Equation 3-31}$$

and

$$\dot{m}_t = \frac{\dot{m}\sqrt{\Theta}}{\delta} \quad \rightarrow \text{(mass flow parameter)} \qquad \textbf{Equation 3-32}$$

- Conservation equations

  Mass balance:

$$\dot{m}_{in} = \dot{m}_{out} \qquad \textbf{Equation 3-33}$$

  Energy balance:

$$\dot{m}_{in} h_{in} = \dot{m}_{out} h_{out} + P_t \qquad \textbf{Equation 3-34}$$

The map which is used in turbine subroutine is taken from reference [41]. The map was scaling using the equations 3-23 and 3-24. The scaled maps are shown in Figure 3-6 and Figure 3-7.

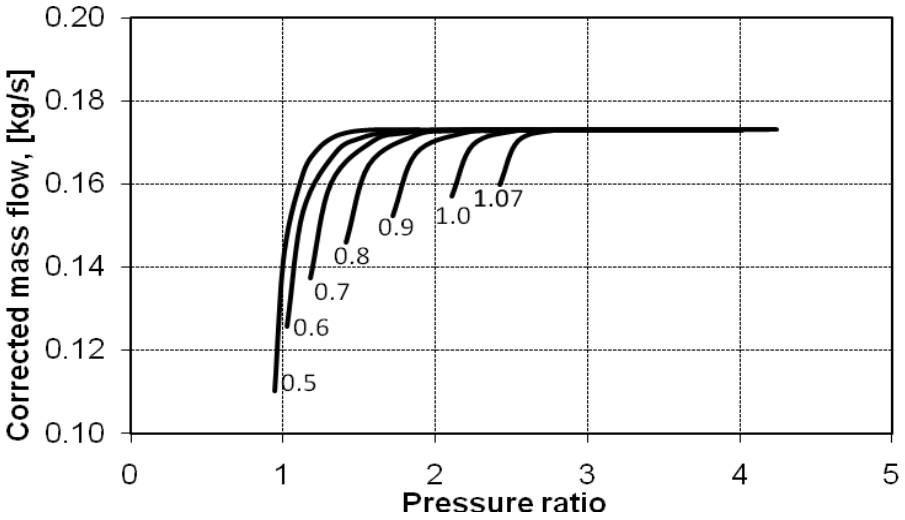

Figure 3-6 Turbine map (mass flow)

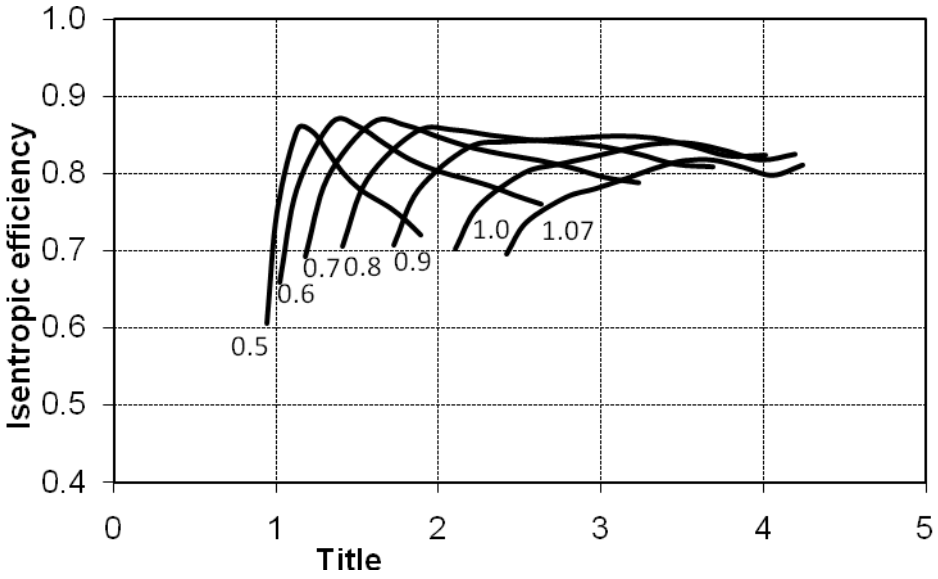

Figure 3-7 Turbine map (efficiency)

3.3.3 Recuperator

In micro turbines, the recuperator is used to preheat the compressed air exit the compressor. The air preheating is led to higher a higher efficiency and less fuel consumption. An AspenPlus heat exchanger module *HeatX* is selected to simulate the heat transfer from hot exhaust gas to colder compressed air.

HeatX can perfom a full zone analysis with heat transfer coefficient and pressure drop estimation for single and two phase streams. The model can be supplied with exchanger geometry for rigorous heat transfer and pressure drop calculations. If exchanger geometry is unknown or unimportant, *HeatX* perform simplified shortcut rating calculations, such as material and heat balance calculations. The *HeatX* block is shown in Figure 3-8.

In our case the heat exchanger geometry is unknown and the block perform simplified calculation given as input the exit temperature of hot stream.

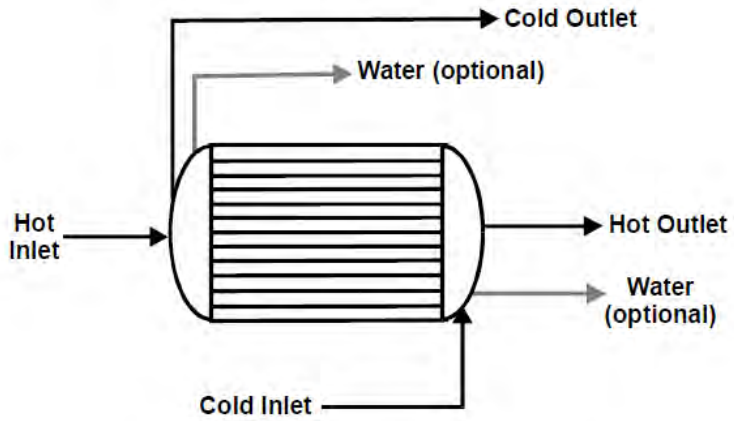

Figure 3-8 AspenPlus *HeatX* block

3.3.4 Burner

In the burner the compressed and preheated air is mixed with the fuel and burned in order to increase its temperature. An AspenPlus stoichiometric reactor *RStoic* is selected to simulate the chemical reaction occurring inside the burner.

The block *RStoic* is used to model a reactor when reaction kinetics are unknown or unimportant and stoichiometry and the molar extend or conversion is known for each reaction. *RStoic* can model reactions occurring simultaneously or sequential. In addition, *RStoic* can perform product selectivity and heat of reaction calculations. In Figure 3-9 is figured the *RStoic* block.

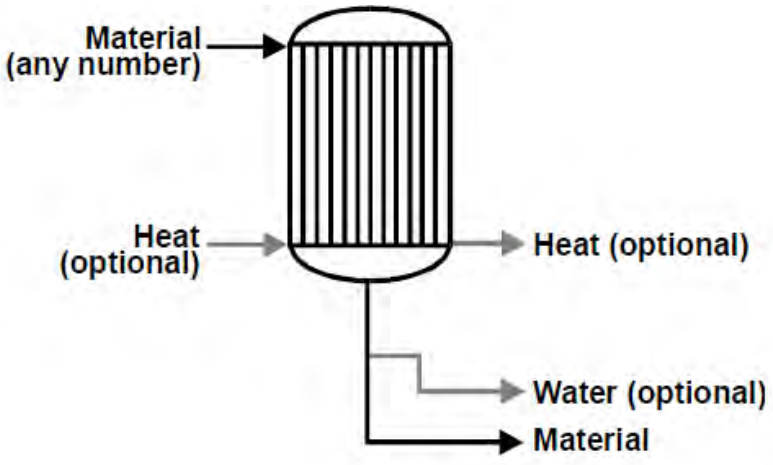

Figure 3-9 AspenPlus *RStoic* block

In our case the inputs to that block are:

- Mass stream
- Flow stream
- Operating pressure
- Chemical reactions
- Head duty

3.3.5 Capstone C30 Model

The blocks described in paragraphs 3.3.1-3.3.4 are placed in a flowsheet and interconnected using material and work streams. The completed flowsheet is presented in Figure 3-10.

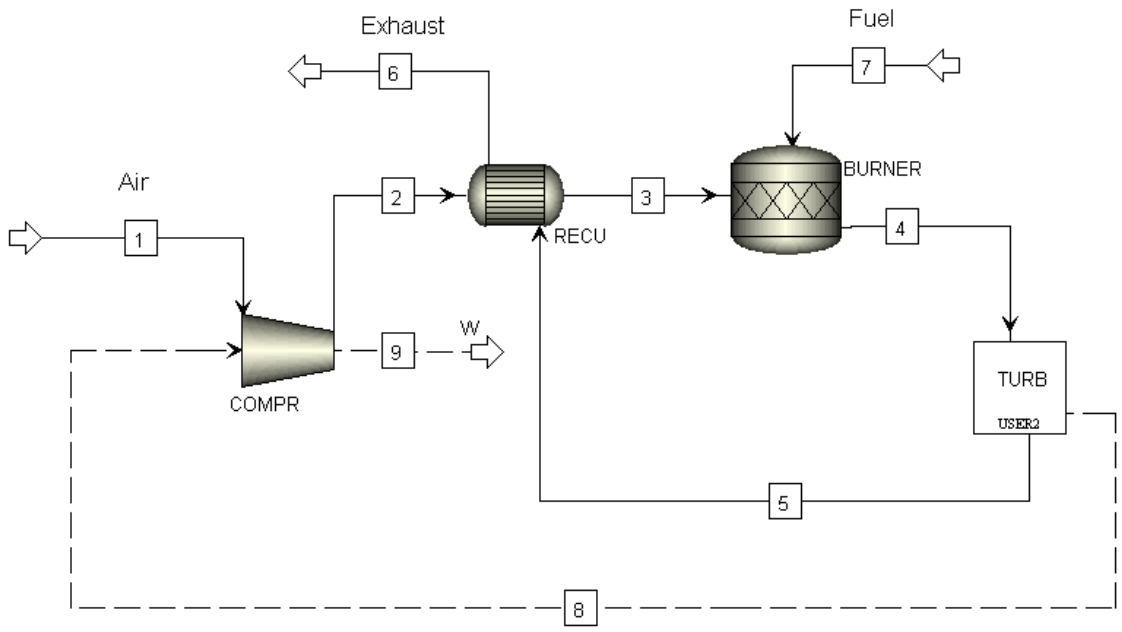

Figure 3-10 Micro turbine model in AspenPlus

The assumptions of the gas turbine model are presented on Table 3-3. The part load operation of the micro turbine is achieved by varying the rotational speed under constant turbine inlet temperature. This control method is preferred in micro turbines since arise higher cycle efficiencies [10].

The inputs to the model are:

- The ambient conditions (temperature, pressure)
- Rotational speed (control variable)

The micro turbine power is calculated as follows, considering mechanical and generator losses.

$$W_{GT} = (W_t \eta_m - W_c)\eta_{gen}$$ **Equation 3-35**

The efficiency of the micro turbine system is given from the following equation

$$\eta_{GT} = \frac{W_{GT}}{\dot{m}_f LHV}$$ **Equation 3-36**

In reference [42], there are data about the part load operation of the Capstone C30 engine. By introducing that data into the simulation model is possible to obtain the remaining parameters.

Pressure ratio	3.6
Turbine inlet temperature	1116.5K
Recuperator Δp/p air/gas side (design point)	2%/3%
Recuperator hot inlet-cold outlet temp. difference	100K
Combustion chamber Δp/p (design point)	2%
Compressor isentropic efficiency (design point)	79.6%
Turbine isentropic efficiency(design point)	84%
Power conditioner system	96%
Mechanical efficiency	97%
Generator efficiency	96%

Table 3-3 Capstone C30 design point data

In the following pictures the basic operating parameter of Capstone C30 engine, as arise from AspenPlus model, are presented and compared with manufacturer data [42]. It is obvious that the developed model predicts very well the engine performance.

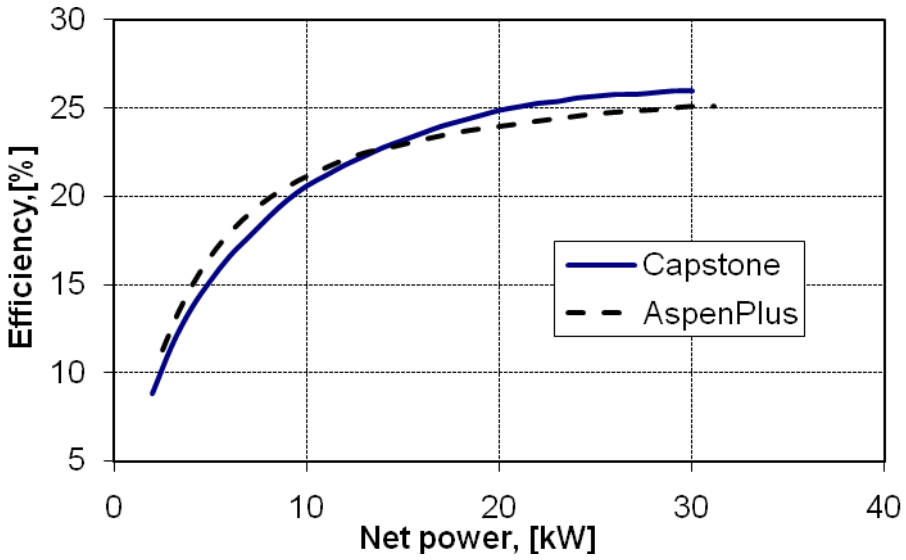

Figure 3-11 Capstone C30 efficiency

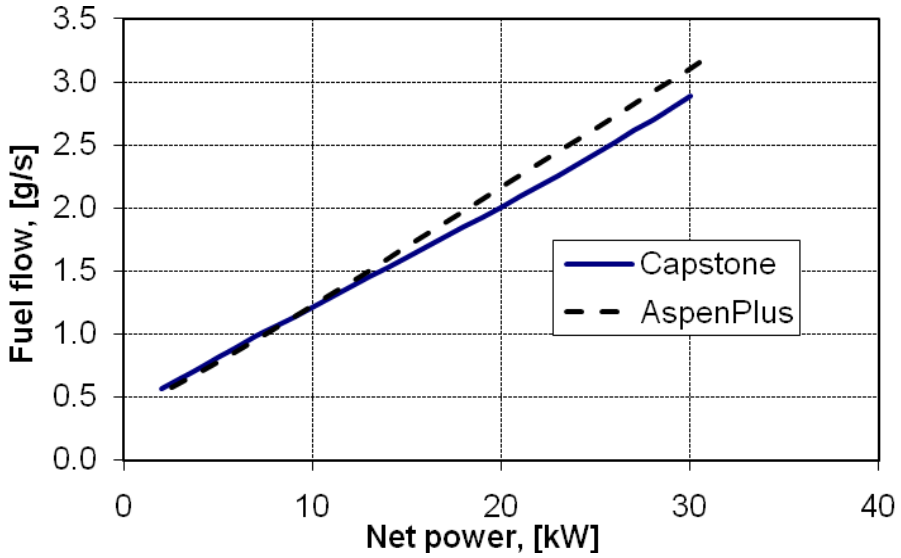

Figure 3-12 Capstone C30 fuel flow

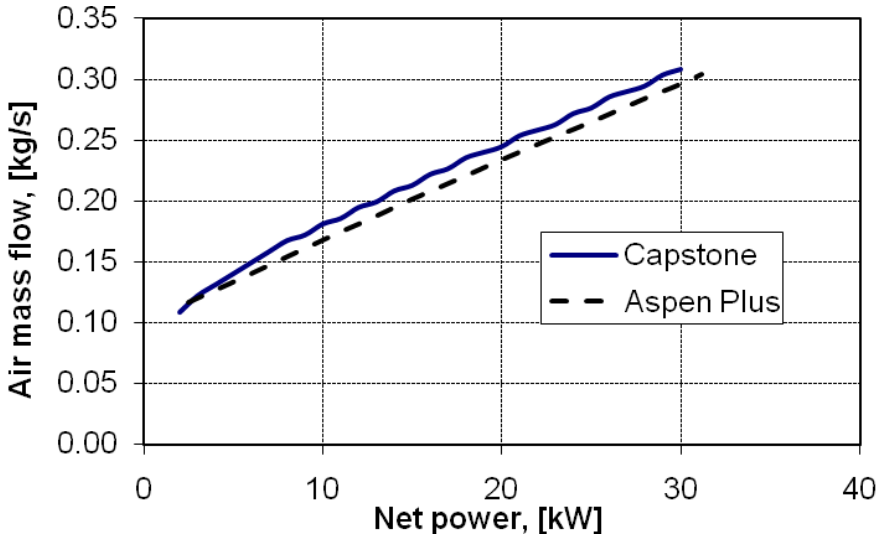

Figure 3-13 Capstone C30 air mass flow

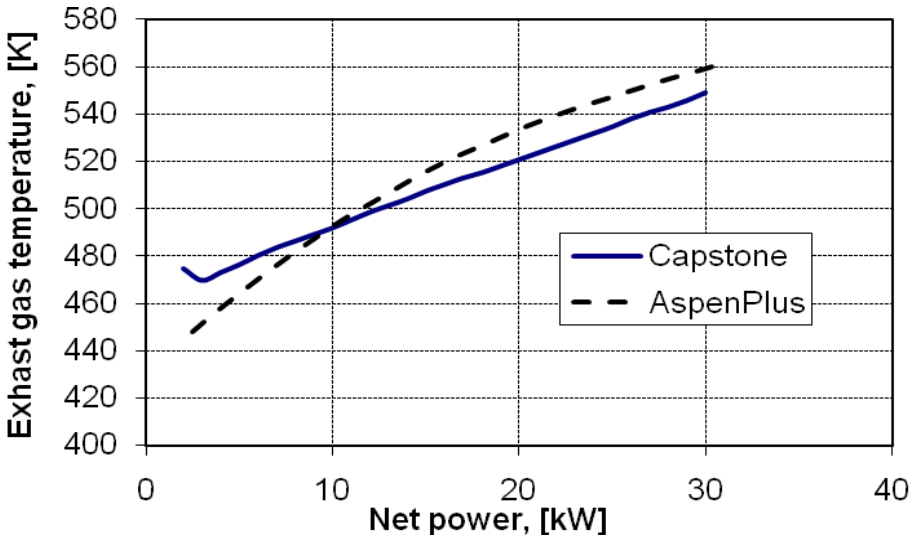

Figure 3-14 Exhaust gas temperature of Capstone C30

3.4 Hybrid system

In Figure 3-15 is presented the developed model of the hybrid system in AspenPlus software. It is basically consists from the recuperative gas turbine engine model which is described in section 3.3.5, where the combustor has been substituted from a SOFC stack

model with was presented in section 3.2. For better supervision the SOFC stack blocks have been introduced to a *Hierarchy* block. The air enters from the compressor where its pressure raises. Thereinafter, the compressed air is preheated in the recuperator and is led in the SOFC stack where reacts electrochemically with the fuel. The hot exhaust gases from the fuel cell stack are expanded on the turbine and produces mechanical work for the compressor and electric generator. The hot gases at the exit of the turbine are used in order to preheat the supplied air to the stack.

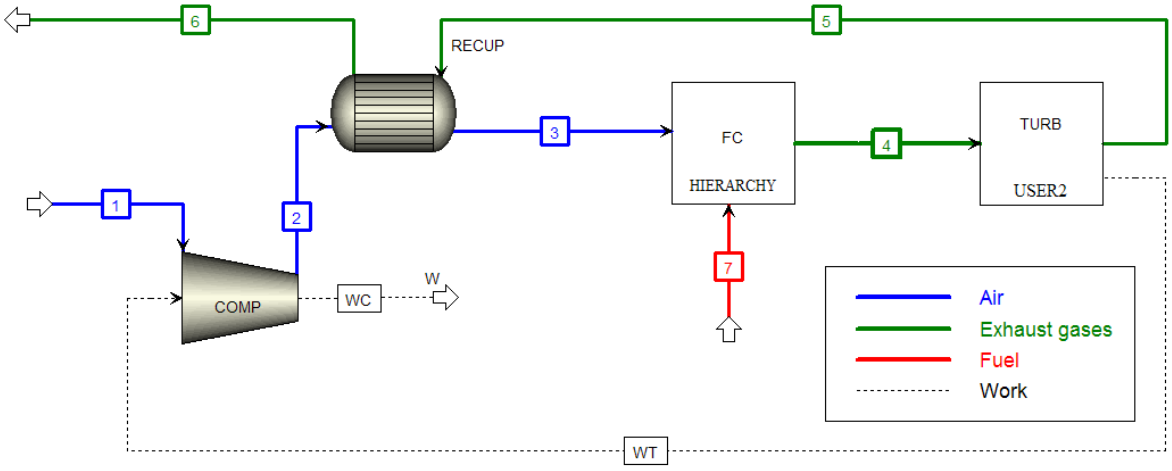

Figure 3-15 Hybrid system modeled in AspenPlus

The final hybrid model incorporates all the assumptions contained in Table 3-1 and Table 3-3. The design point of the plant is defined based on these assumptions. The relevant data are presented in Table 3-4.

Total power	206 kW
SOFC power	172 kW
GT power	33 kW
Fuel consumption	8.1173 g/s
Air flow	0.295 kg/s
Exhaust gas temperature	884 K
Efficiency	65.8 %
Fuel cell efficiency	55.2 %

Table 3-4 Hybrid system design point data

The part-load operation of the hybrid system is made by varying the micro turbine rotational speed. However in order to implement a certain operation strategy, also SOFC temperature, turbine inlet temperature and fuel utilization factor have to be determined.

The output power of the hybrid system is estimated from the following equation:

$$W_{HS} = W_{SOFC} + W_{GT}$$ **Equation 3-37**

The power generation efficiency of the SOFC and the hybrid system are defined, respectively, as:

$$\eta_{SOFC} = \frac{W_{SOFC}}{\dot{m}_f LHV}$$ **Equation 3-38**

$$\eta_{HS} = \frac{W_{HS}}{\dot{m}_f LHV}$$ **Equation 3-39**

4. Simulation results and analysis

In the following paragraphs the part load behavior of hybrid system is presented and the effects of various performance parameters are examined. In this study the controlled variables are the rotational speed, the SOFC temperature, the turbine inlet temperature and the fuel utilization factor. The manipulated variables for control purposes are the fuel mass flow, the air mass flow and the recycle ratio.

4.1 Hybrid system part-load performance

In that section the part load performance obtained by varying only the rotational speed of the micro-turbine. The other operating variables are fixed, in order to simplify the system analysis.

As shown in Figure 4-1 the total power output of the hybrid system increases linear with the micro turbine rotational speed as expected for that type of thermal systems [43].

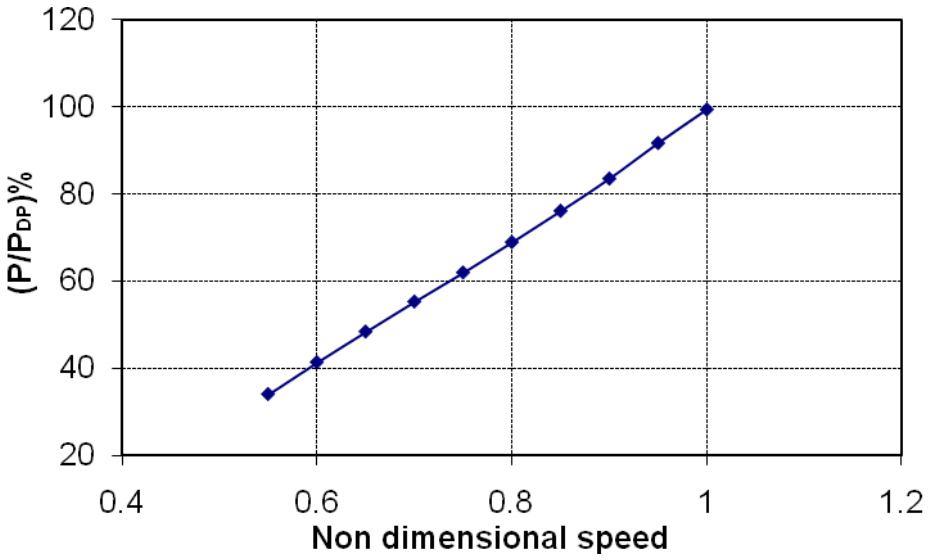

Figure 4-1 Total power production vs. non dimensional rotational speed

In Figure 4-2 is presented the total system efficiency as a function of the non dimensional power output. The system efficiency increases when the system operates at part load. The

maximum efficiency is achieved at a load of about 40% of the nominal operating power. This is occurs because of the recuperator effectiveness increases significantly with decreasing of air mass flow under variable rotational speed operation, [5].

The air mass flow increases nearly linear with the total power (Figure 4-3) since there is a linear relation between the power output and the rotational speed. Under variable rotational speed the air mass flow is change according the operating line of the centrifugal compressor.

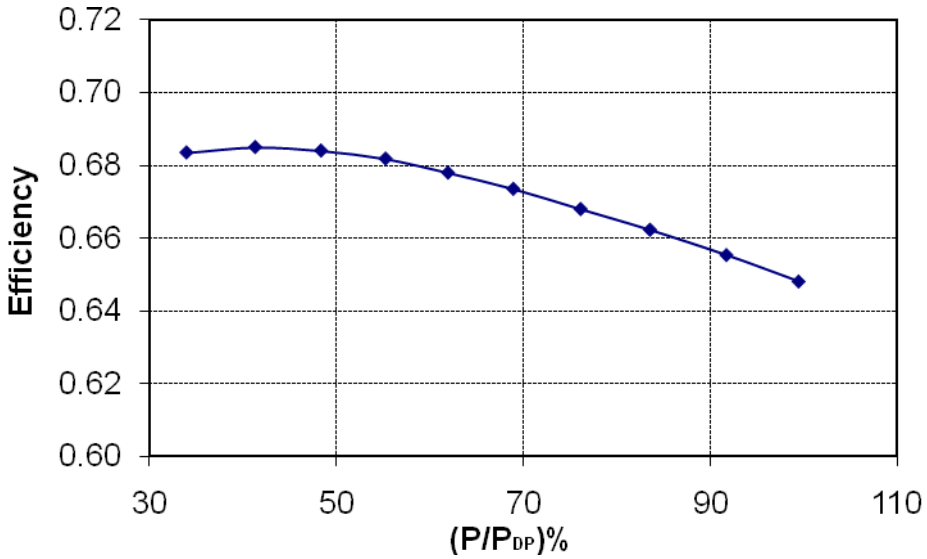

Figure 4-2 Part load performance of hybrid system

Figure 4-3 presents the oxygen utilization factor in the cathodic electrode. The results of present work are in a good agreement with previous works [5, 43, 44] although assumes different fuel utilization factors. This means that the ratio of the air flow rate to the fuel consumption is almost comparable among all the cited results, [43].

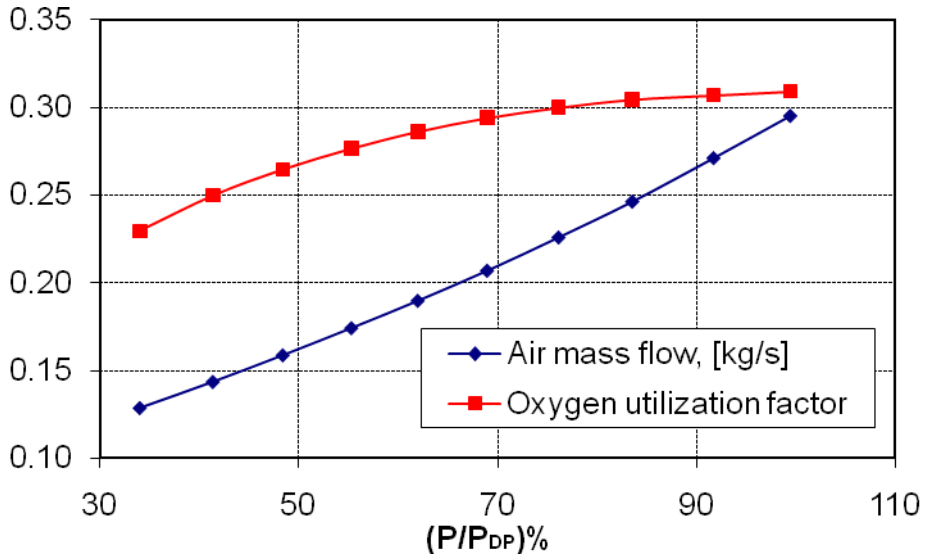

Figure 4-3 Air mass flow and oxygen utilization factor vs. power output

In Figure 4-4 is shown the characteristic curve of the fuel cell. The design point values of the current density (2670 A/m^2) and the fuel cell voltage (about 0.7 V) match with the results of Kimijima and Kasagi, [43].

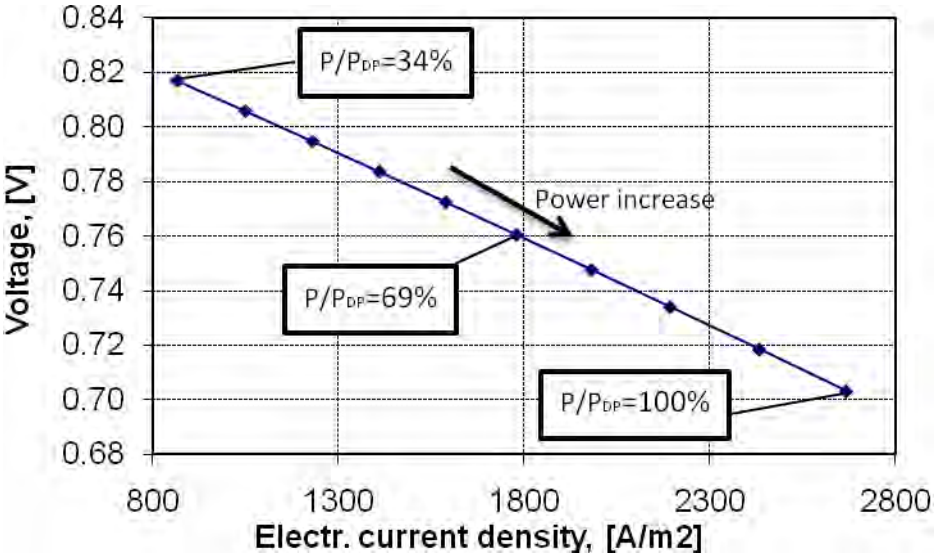

Figure 4-4 Fuel cell characteristic curve

The compressor outlet temperature (Figure 4-5) increases with the power output due to the increment of pressure ratio. On the other hand, the compressed air exits with higher temperature, compared with design point, from the recuperator when the system operates part load. This is because of the increased turbine outlet temperature at low loads (Figure 4-6) and the improved recuperator effectiveness by the reduction of air flow rate.

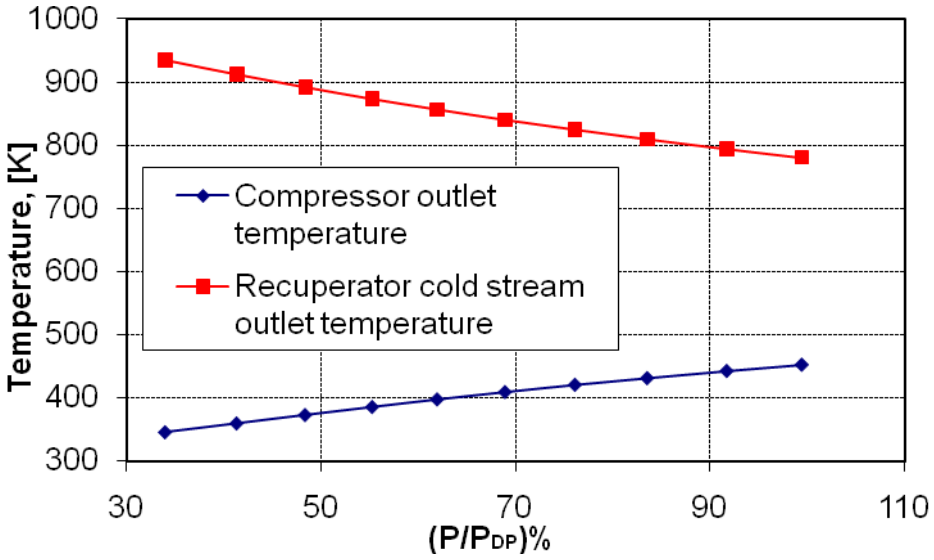

Figure 4-5 Compressor and recuperator cold stream outlet temperatures

As shown in the following picture, under part load operation the turbine outlet temperature increase due to the reduction of the pressure ratio and air mass flow in turbine component [43]. On the contrary, the exhaust gas temperature decreases, since the recuperator works more efficiently and absorbs more heat energy from the hot exhaust.

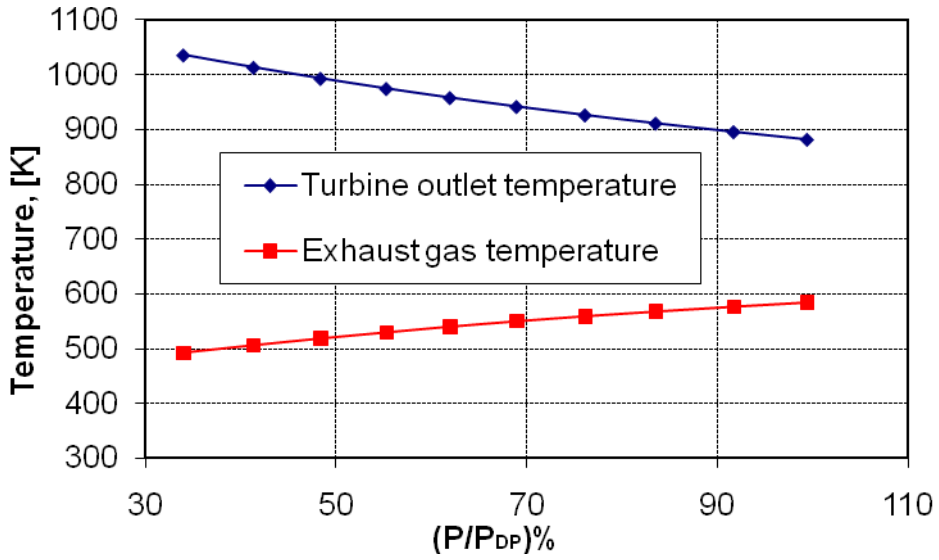

Figure 4-6 Temperature of exhaust gas and at turbine outlet

Regarding to the SOFC stack efficiency, it increases when the system operates at part-load (Figure 4-7), due to reduced ohmic losses ant increased air inlet temperature (Figure 4-5). Also, as shown in the following graph, there is a linear relationship between the fuel consumption and the power output, [43].

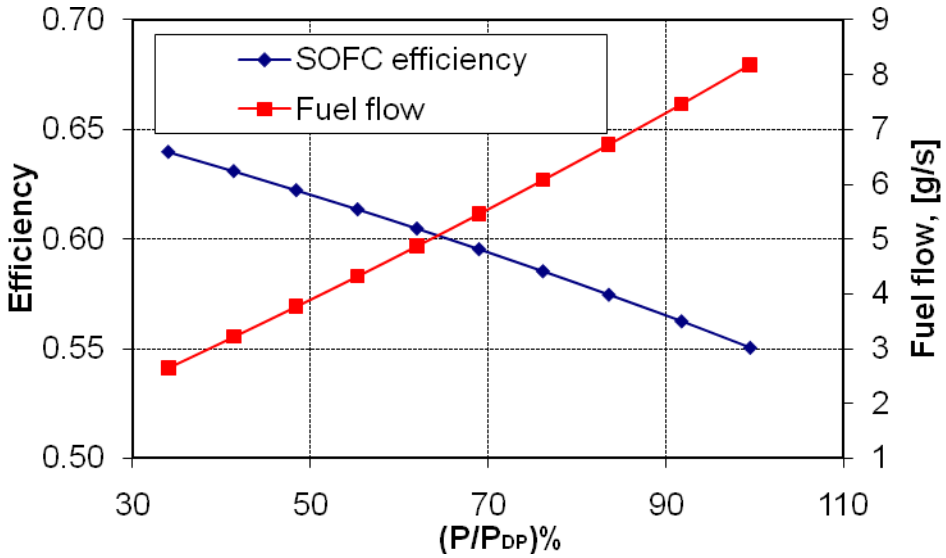

Figure 4-7 SOFC stack efficiency and fuel flow

In Figure 4-8 are presented the turbomachineries efficiencies. It is obvious that turbine isentropic efficiency has nearly constant value, about 85%, whilst the compressor efficiency decreases as the power decrease and takes a constant value of about 73%.

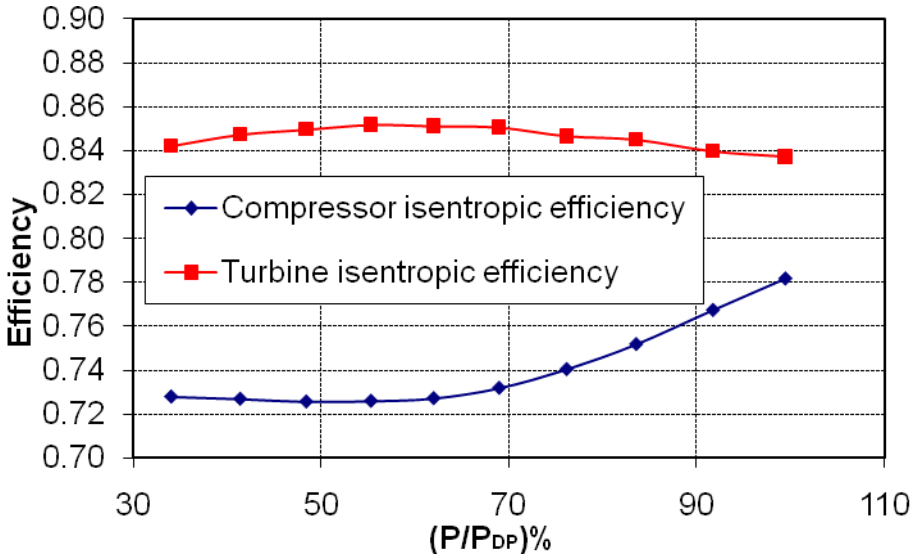

Figure 4-8 Turbomachineries efficiencies

Finally, in Figure 4-9 is presented the micro turbine to SOFC group power ratio at part load condition. The power ratio between micro turbine and fuel cell stack is 18% at the hybrid system design point and decreases nearly linear with the total power output.

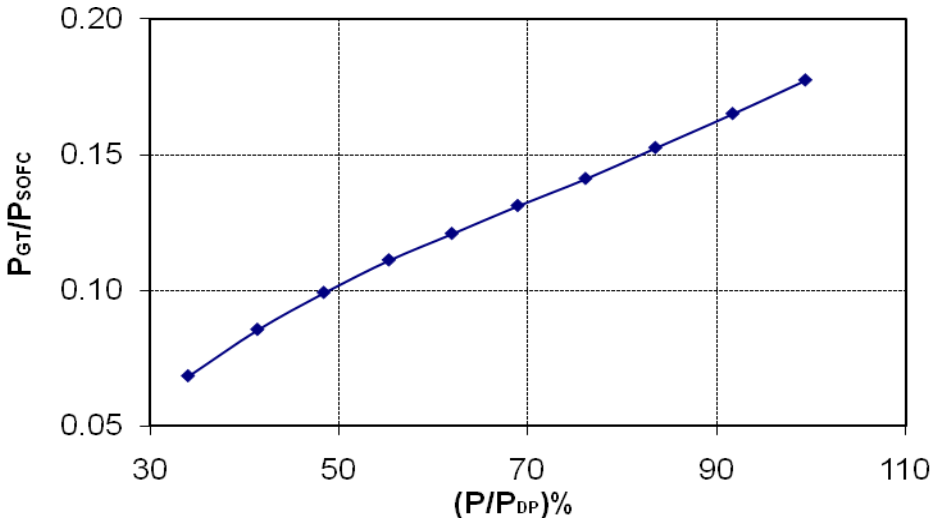

Figure 4-9 Micro turbine to SOFC group power ratio at part load conditions

4.2 Effect of turbine inlet temperature

In the presented model the turbine inlet temperature is a performance parameter which controlled from the user. In Figure 4-10 is presented the part load behavior of the system for various values of turbine inlet temperature. The system works more efficiently for the higher values of turbine inlet temperature. Also, the system efficiency increases along the curves for constant turbine inlet temperature, due to the improved performance of the recuperators since they operate with lower mass flows.

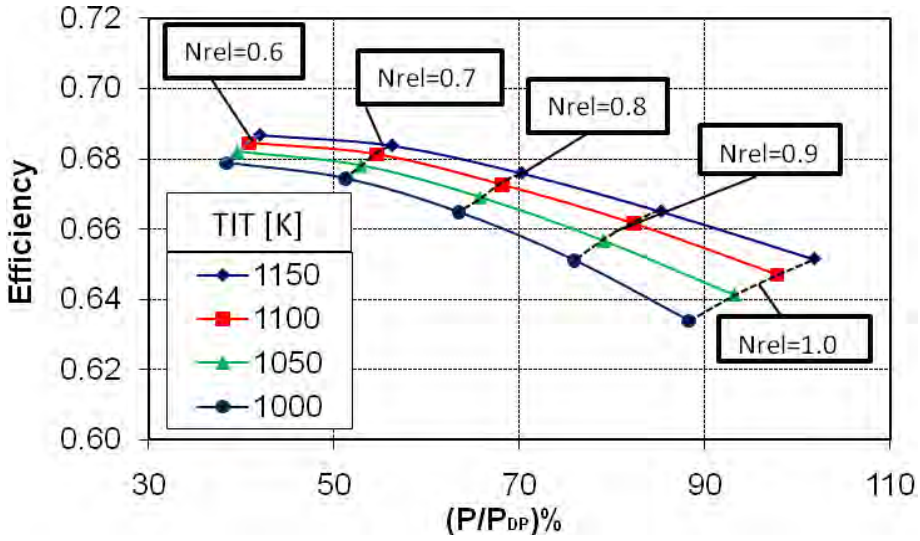

Figure 4-10 Hybrid plant system efficiency vs. non-dimensional power (T_{SOFC} = 1183.5 K, U_f = 0.85, SCR=2.5)

The effect of turbine inlet temperature in various operating parameters is presented in Figure 4-11. The results arise for three values of rotational speed – 100% (high), 80% (medium) and 60% (low) of nominal rotational speed – by increasing the turbine inlet temperature 1 percent and calculating the deviations according to Eq. 3-40.

$$Deviation[\%] = 100 \cdot \frac{X_{new} - X_{reference}}{X_{reference}} \qquad \textbf{Equation 3-40}$$

The subscript -*new* refers to the values result after the operating parameter increment and the subscript -*reference* refers to the initial values without the operating parameter increment.

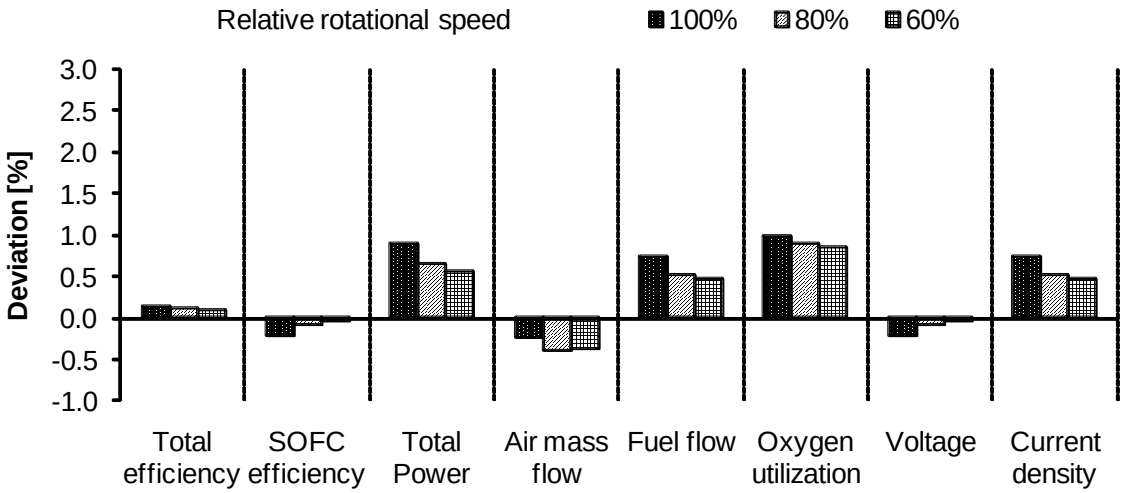

Figure 4-11 Effect of turbine inlet temperature

Figure 4-11 present the effect of turbine inlet temperature on various system operating parameters. The increment of turbine inlet temperature slightly increases the total efficiency of the hybrid system, this is because larger amount of energy expanded in the turbine and produce more power. On the other hand, the SOFC stack efficiency decreases since smaller amount of thermal energy of the exhaust gases is used to preheat the fresh air, as a result, the air enters with lower temperature in the cathode side of fuel cells. The increment of turbine inlet temperature causes the system to consume more fuel in order to maintain the higher value of the temperature. The turbine inlet temperature affects the matching of turbomachinery components, this fact contribute to a decrease of the air flow enters the compressor. As it can be seen in Figure 4-11 the oxygen utilization factor increases, since more oxygen needed, in order to oxidize the increased fuel flow, also, this causes higher values of current density. The fuel cell voltage (as the SOFC efficiency) decreases, because the fuel utilization factor was kept constant.

4.3 Effect of SOFC stack temperature

The SOFC temperature is one of the most important operating parameters for fuel cells and hybrid systems since has significant effects in power and efficiency. In Figure 4-12 it is obvious that when the micro turbine operates at constant rotational speed a reduction in fuel cell temperature contribute to lower efficiencies and lower power production. The drop is higher when compared with Figure 4-10 where a reduction of turbine inlet temperature of 150 K contributes to the decrease of system efficiency of about 2%. On the other hand, a reduction of fuel cell temperature of 60 K, causes a decrease of system efficiency of about 4%.

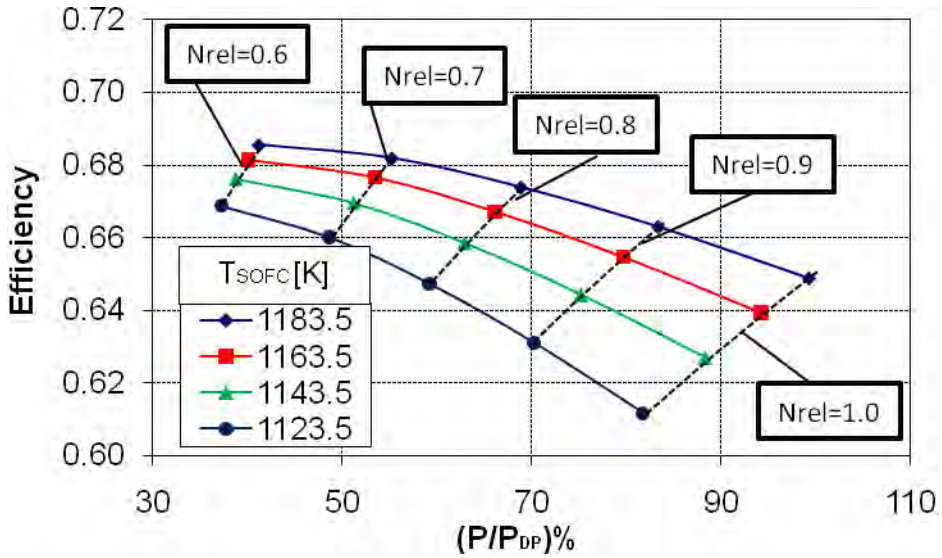

Figure 4-12 Hybrid plant system efficiency vs. non-dimensional power (TIT = 1117 K, U_f = 0.85, SCR=2.5)

In order to study the effect of SOFC temperature on various operating parameters we follow the same procedure as in section 4.2.

As it can be seen in Figure 4-13 the higher SOFC temperature makes the system to operate more efficiently. The increment in SOFC stack efficiency is owing to the lower losses (electrical resistance) in high temperatures [5]. The lower losses cause the SOFC stack to

produce more power with higher operating voltage. The fuel flow increases in order to maintain the higher stack temperature. Contrary to the impact of turbine inlet temperature, the fuel cell temperature does not affect (siglificantly) the amount of air mass flow since does not perturb the matching of turbomachinery components. With reference to the oxygen utilization factor, its value increases, since more oxygen needed, in order to oxidize the increased fuel flow.

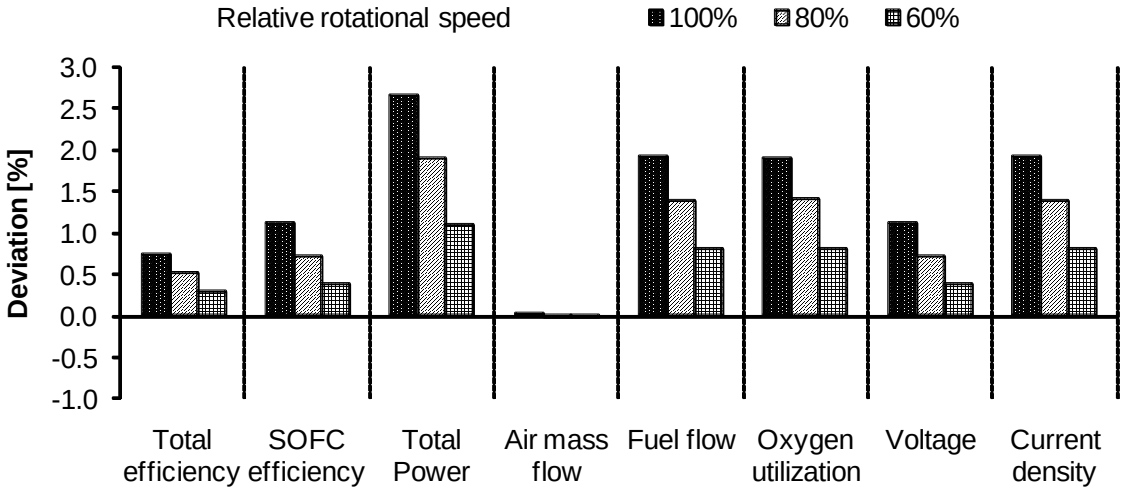

Figure 4-13 Effect of SOFC temperature

4.4 Effect of fuel utilization factor

The plant efficiency increases as the fuel cell utilization factor increase, because of the more effective operation of fuel cell stack (Figure 4-14). The profit of fuel utilization factor increment is larger when the system operates at off design points, as it is shown in Figure 4-14 where the curves of constant fuel utilization factor diverge as the power output decrease.

The increment of fuel utilization factor makes the hybrid system operates more efficiently too. As it can be seen in Figure 4-15 the fuel utilization factor affects the system more, when it operates with low rotational speed, in contrast to the other operating parameters (TIT and T_{SOFC}). The behavior of the operating parameters shown in the following figure is similar with the Figure 4-13. The only difference is that the fuel cell voltage decrease due to the large increment current density witch result larger electrical resistance losses in the cell.

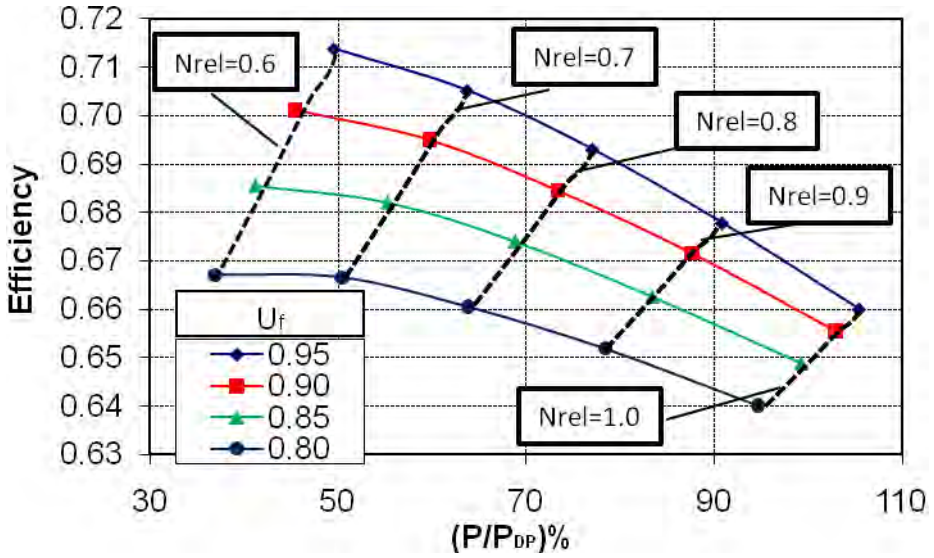

Figure 4-14 Hybrid plant system efficiency vs. non-dimensional power (TIT = 1117 K, T_{SOFC} = 1183.5K , SCR=2.5)

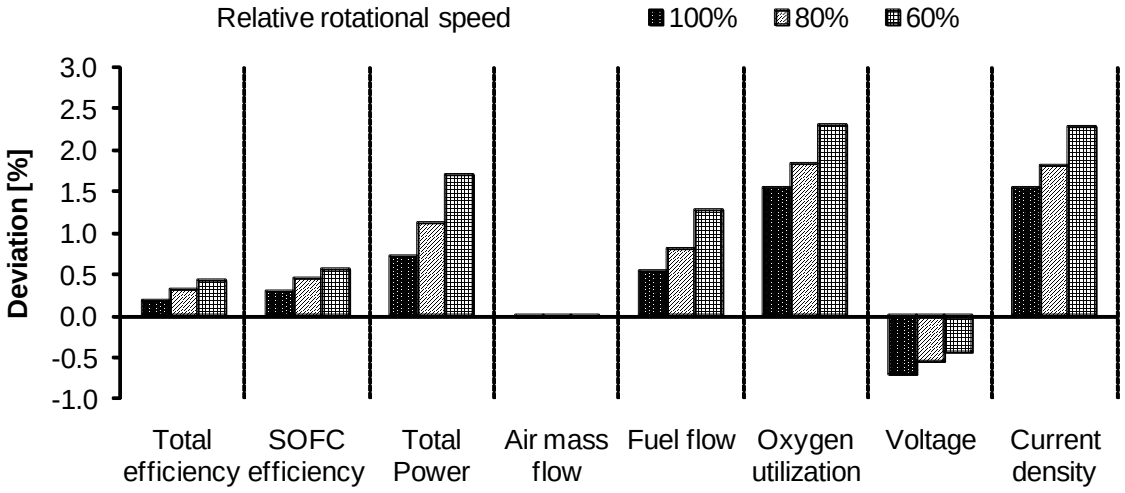

Figure 4-15 Effect of fuel utilization factor

5. Conclusions and recommendations

The objective of this thesis was to develop a simulation model for a small scale hybrid SOFC-GT system, based on actual devices. The fuel cell model was based on the tubular configuration developed by Siemens Power Generation Inc. Although, the selected software did not have a model for the basic SOFC stack, an alternative approach was implemented in order to develop a SOFC model.

The micro turbine selected is the commercial available Capstone C30. A model was developed using general performance maps and available operating data from the manufacturer.

The previous two systems were coupled together, in order to set up a small scale hybrid system, appropriate for microcogeneration applications. The results shown that the two systems can be operate together very efficiently. The power and efficiencies achieved are very high even if the system operates at part load conditions. The increment of the turbine inlet temperature, the SOFC temperature and fuel utilization factor have a positive impact on overall system performance.

The high temperature of exhaust gases shown that can be used in order to drive thermally activated devices.

Further improvements are going to be done, such as the integration with devices to produce cooling and heating for buildings.

6. References

[1] Oliver JR. A micro-Cooling, Heating and Power (m-CHP) instructional module. Department of Mechanical Engineerin, vol. Master thesis. Mississippi: Mississippi State University, 2005.

[2] Onovwiona HI, Ugursal VI. Residential cogeneration systems: review of the current technology. Renewable and Sustainable Energy Reviews 2006;10:389.

[3] Wu DW, Wang RZ. Combined cooling, heating and power: A review. Progress in Energy and Combustion Science;32:459.

[4] Technology Characterization: Microturbines. vol. USA:Environmental Protection Agency: Energy Nexus Group, 2002.

[5] Costamagna P, Magistri L, Massardo AF. Design and part-load performance of a hybrid system based on a solid oxide fuel cell reactor and a micro gas turbine. Journal of Power Sources 2001;96:352.

[6] Adrian V, Joan Carles B, Roberto B, Alberto C. Performance characteristics and modelling of a micro gas turbine for their integration with thermally activated cooling technologies. vol. 31, 2007. p.119.

[7] Kim TS, Hwang SH. Part load performance analysis of recuperated gas turbines considering engine configuration and operation strategy. Energy;31:260.

[8] Nascimento MAR, Lora ES, Corrкa PSP, Andrade RV, Rendon MA, Venturini OJ, Ramirez GAS. Biodiesel fuel in diesel micro-turbine engines: Modelling and experimental evaluation. Energy 2008;33:233.

[9] NATO Research and Technology Organization, Performance prediction and simulation of gas turbine engine operation for aircraft, marine, vehicular, and power generation: RTO-TR-044, 2002.

[10] Wang W, Cai R, Zhang N. General characteristics of single shaft microturbine set at variable speed operation and its optimization. Applied Thermal Engineering 2004;24:1851.

[11] Fuel Cell Handbook. vol. US: Department of energy, 2000.

[12] Gou B, Na WK, Diong B. Fuel Cells: Modeling, Control and Applications: CRC Press, 2010.

[13] Larmine J, Dicks A. Fuel Cells Systems Explained: John Wiley & Sons Ltd, 2003.

[14] Stiller C. Design, Operation and Control Modelling of SOFC/GT Hybrid Systems. Department of Enegry and Process Engineering: Norwegian University of Sciencce and Technology, March 2006.

[15] Zhang W, Croiset E, Douglas PL, Fowler MW, Entchev E. Simulation of a tubular solid oxide fuel cell stack using AspenPlusTM unit operation models. Energy Conversion and Management 2005;46:181.

[16] Campanari S, Iora P. Definition and sensitivity analysis of a finite volume SOFC model for a tubular cell geometry. Journal of Power Sources 2004;132:113.

[17] Song TW, Sohn JL, Kim JH, Kim TS, Ro ST, Suzuki K. Performance analysis of a tubular solid oxide fuel cell/micro gas turbine hybrid power system based on a quasi-two dimensional model. Journal of Power Sources 2005;142:30.

[18] Stiller C, Thorud B, Seljebψ S, Mathisen Ψ, Karoliussen H, Bolland O. Finite-volume modeling and hybrid-cycle performance of planar and tubular solid oxide fuel cells. Journal of Power Sources 2005;141:227.

[19] Campanari S. Thermodynamic model and parametric analysis of a tubular SOFC module. Journal of Power Sources 2001;92:26.

[20] Hassmann K. SOFC Power Plants, the Siemens-Westinghouse Approach. Fuel Cells 2001;1:78.

[21] Singhal CS, Kendal K. High Temperature Solid Oxide Fuel Cells: Fundamentas, Design and Applications: Elsevier, 2003.

[22] George RA. Status of tubular SOFC field unit demonstrations. Journal of Power Sources 2000;86:134.

[23] Fuel cell related web site of Siemens. http://www.energy.siemens.com, vol. June.

[24] Layne A, Samuelsen S, Williams M, Holcombe N. Hybrid Fuel Cell Heat Engines: Recent Efforts. ASME paper GT2001-0588.

[25] Stephen EV, Shailesh DV, Kavin PL, Wayne LL. Status of Pressurized SOFC/Gas Turbine Power System Development at Siemens Westinghouse. ASME paper GT2002-30670.

[26] AspenPlus 11.1 User Guide: AspenTech Ltd, 2001.

[27] Adriαn V, Joan Carles B, Roberto B, Alberto C. Performance characteristics and modelling of a micro gas turbine for their integration with thermally activated cooling technologies. vol. 31, 2007. p.119.

[28] Zheng L, Furimsky E. ASPEN simulation of cogeneration plants. Energy Conversion and Management 2003;44:1845.

[29] Kuchonthara P, Bhattacharya S, Tsutsumi A. Energy recuperation in solid oxide fuel cell (SOFC) and gas turbine (GT) combined system. Journal of Power Sources 2003;117:7.

[30] Pangalis MG, Martinez-Botas RF, Brandon NP. Integration of solid oxide fuel cells into gas turbine power generation cycles. Part 1: fuel cell thermodynamic modelling. Proceedings of the Institution of Mechanical Engineers -- Part A -- Power & Energy 2002;216:129.

[31] Palsson J, Selimovic A, Sjunnesson L. Combined solid oxide fuel cell and gas turbine systems for efficient power and heat generation. Journal of Power Sources 2000;86:442.

[32] Riensche E, Stimming U, Unverzagt G. Optimization of a 200 kW SOFC cogeneration power plant Part I: Variation of process parameters. Journal of Power Sources 1998;73:251.

[33] Meyer L, Tsatsaronis G, Buchgeister J, Schebek L. Exergoenvironmental analysis for evaluation of the environmental impact of energy conversion systems. Energy 2009;34:75.

[34] Doherty W, Reynolds A, Kennedy D. Modelling and simulation of a biomass gasification-solid oxide fuel cell combined heat and power plant using Aspen Plus. 22nd International Conference on Efficiency, Cost, Optimization, Simulation and Environmental Impact of Energy Systems, 2009.

[35] Fuller EN, Schettler PD, Giddings JC. A new method for prediction of binary gas-phase diffusion coefficients. Industrial & Engineering Chemistry 1966;58:18.

[36] Kautz M, Hansen U. The externally-fired gas-turbine (EFGT-Cycle) for decentralized use of biomass. Applied Energy 2007;84:795.

[37] Ong'iro A, Ugursal VI, Al Taweel AM, Lajeunesse G. Thermodynamic simulation and evaluation of a steam CHP plant using ASPEN Plus. Applied Thermal Engineering 1996;16:263.

[38] Boyce M. Gas turbine engineering handbook: Butterworth-Heinemam, 2002.

[39] Kong C, Ki J, Kang M. A New Scaling Method for Component Maps of Gas Turbine Using System Identification. Journal of Engineering for Gas Turbines and Power 2003;125:979.

[40] Bakalis D, Stamatis A. Extended instrumentation and model calibration for a small micro-turbine. ASME paper GT2010-22837.

[41] Stiller C. Design, Operation and Control Modelling of SOFC/GT Hybrid Systems. Norwegian University of Science and Technology: PhD thesis, 2006.

[42] Technical Reference: Capstone Model C30 Performance: Capstone Turbine Corporation, Rev. D (April 2006).

[43] Kimijima S, Kasagi N. Performance Evaluation of Gas Turbine-Fuel Cell Hybrid Micro Generation System. ASME paper GT2002-30111.

[44] Campanari S. Full Load and Part-Load Performance Prediction for Integrated SOFC and Microturbine Systems. Journal of Engineering for Gas Turbines and Power 2000;122:239.